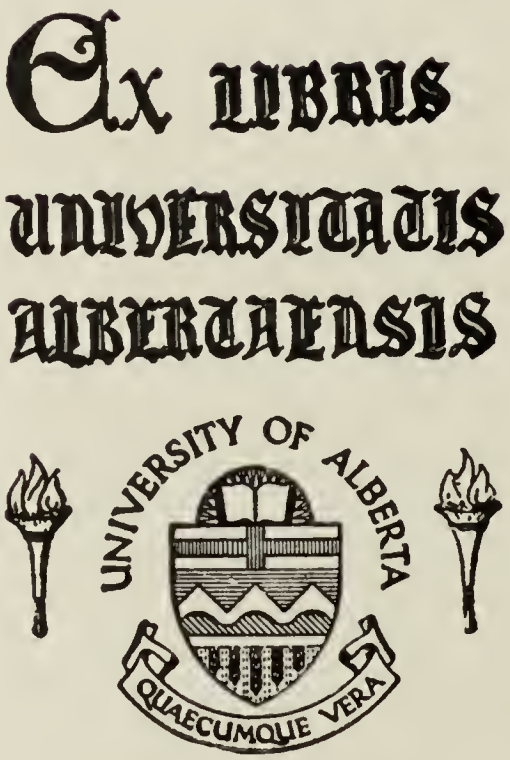

University of Alberta
Printing Department

THE UNIVERSITY OF ALBERTA

INVESTIGATION OF RHEOLOGICAL CHARACTERISTICS OF SAND-WATER SUSPENSIONS

by

K. SUBRAMANYA, B.E., M.Sc.(Engg).

A THESIS

SUBMITTED TO THE FACULTY OF GRADUATE STUDIES
IN PARTIAL FULFILMENT OF THE REQUIREMENTS
FOR THE DEGREE OF

MASTER OF SCIENCE

DEPARTMENT OF CIVIL ENGINEERING

EDMONTON, ALBERTA

August, 1965

UNIVERSITY OF ALBERTA

FACULTY OF GRADUATE STUDIES

The undersigned certify that they have read, and recommend to the Faculty of Graduate Studies for acceptance, a thesis entitled

"INVESTIGATION OF RHEOLOGICAL
CHARACTERISTICS OF SAND-WATER SUSPENSIONS"

submitted by

Subramanya Kanakatti

in partial fulfilment of the requirements for the degree of

Master of Science

ABSTRACT

A capillary viscometer was developed to investigate the rheological behaviour of sand-water suspensions.

The suspension was found to behave as a non-Newtonian dilatant fluid over the range of shear rates tested. Bagnold's concept of grain shear stress τ_s and linear concentration λ are used in dimensional analysis of the flow situation. The dimensionless numbers $G_T^2 = \frac{\tau_s \rho_s d^2}{\lambda \eta^2}$ and $\left(\frac{8V}{D}\right)\frac{\rho_s d^2}{\eta}$ are found to bear unique functional relationship for all values of $\lambda < 3.5$. By comparison with the experimental observation of Bagnold, the existence of a critical G_T^2 is postulated such that the $G_{T_{cr}}^2$ marks the transition from Newtonian to non-Newtonian flow regime.

A critical concentration at which there is an abrupt change in the characteristics of the suspension is noticed at concentrations between 0.30 and 0.35.

ACKNOWLEDGMENTS

The author is grateful to Dr. T. Blench for his valuable guidance and encouragement throughout the course of this program.

Thanks are due to Dr. M.P. Duplessis for his, assistance in developing the viscometer, encouragement and helpful discussions.

Grateful acknowledgment is made to Prof. A.W. Peterson and to the staff of the Hydraulics laboratory for their help in various phases of the work.

The author is thankful to the Government of Canada for awarding him a Commonwealth Scholarship which made this study possible.

TABLE OF CONTENTS

LIST OF TABLES

LIST OF FIGURES

LIST OF FIGURES - continued

NOMENCLATURE

a = free distance between adjacent spheres in sec. 2.3

a, A_1, A_2 = constants

b = ratio of the distance between two spheres to the diameter in sec. 2.3

C = volumetric concentration = $\frac{\text{volume of solids}}{\text{volume of suspension}}$

C_* = maximum value of C

C_{cr} = critical concentration

d = diameter of solid particals in suspension

D = diameter of the pipe

E = rigidity modulus

f = friction factor (dimension less)

$f( )$, $fn( )$ = unspecified functional relationship

g = acceleration due to gravity

$g( )$ = unspecified functional relationship

G_T^2 = dimensionless number containing τ_s

G_P^2 = dimensionless number containing p_s

$G_{T_{cr}}^2$ = critical value of G_T^2

H = Hedstrom number

H_m = differential pressure head (measured)

K, K_1, K_2, K' = constants

L = length of capillary tube

m = mass of spheres in sec. 2.3

NOMENCLATURE - continued

m	= exponent in equn. (51)
n	= flow behavior index
n'	= exponent in equn. 22
N	= dimensionless number defined in sec. 2.3
p	= pressure
Δp	= differential pressure
p_s	= repulsive pressure due to grains
Q	= discharge
r	= radial distance
R_e	= Reynolds number
R_e'	= generalised Reynolds number
R_{em}	= modified Reynolds number
R_{e*}	= Shear Reynolds number
S	= constant in equn. (31)
$s( )$	= unspecified functional relationship
t	= time
u, U	= local velocity
u_*	= shear velocity
V	= average velocity
$\frac{8V}{D}$	= flow function
w_h	= hindered settling velocity
w_f	= free settling velocity
y	= length in specified direction
Y	= Yield number
α	= angle of collision of particles in sec. 2.3 = the angle the line of centers makes with the Y direction.

NOMENCLATURE - continued

α = calibration coefficient in equn. (36)

$\dot{\gamma}$ = shear rate = $\frac{du}{dy}$

η = coefficient of dynamic viscosity of the Newtonian liquid

η_a = apparent viscosity

η_r = relative viscosity

η_p = coefficient of rigidity of Bingham-plastic fluid

λ = linear concentration

ν = kinematic viscosity of the Newtonian liquid

ϵ = thickness of anomalous flow

ϵ = (1 - C) in equn. (42)

ρ = density

ρ_f = density of the liquid (suspending medium)

ρ_s = density of the solids

τ = shear stress

τ_f = shear stress due to flow of the liquid medium alone

τ_s = shear stress due to solids

τ_w = shear stress at the wall of the pipe

τ_{wm} = observed wall shear stress

τ_y = Yield shear stress of a Bingham-plastic fluid

τ_t = total shear stress in viscous region, (section 2.3)

$\Sigma()$ =

$\psi()$ = unspecified functional relationship

$\phi()$ =

V = volume

CHAPTER I

INTRODUCTION

1.1 NON-NEWTONIAN FLOW

In recent years there has been a marked increase in interest in the flow and related behaviour of complex mixtures, especially of solid-liquid suspensions. Hydraulic transport of solids is used extensively in road and dam construction, land and harbour reclamation, in mining and chemical industries. In connection with the research investigations or design work on the problems of hydraulic transport a knowledge of the consistency or the "viscosity" of the suspension is usually called for. However, most of the suspensions happen to be non-Newtonian in character. The study of the rheological behaviour of non-Newtonian fluids in general and the suspensions in particular is an extremely complex and incompletely understood field. Advances are being made in the various disciplines.

The object of the present investigation is to study certain aspects of the rheological behaviour of sand-water suspensions. To understand the present status of the knowledge in this topic, it is necessary to know the characteristic behaviour of non-Newtonian fluids. A brief review of non-Newtonian fluid flow is given in this chapter.

1.2 NON-NEWTONIAN FLUIDS:

The behaviour of fluids when subjected to shear stress forms the basis for classifying the fluids into Newtonian and non-Newtonian categories.

Fluids for which the shear rate is directly proportional to the imposed shear stress only are known as Newtonian fluids. The rheological equation is

$$\frac{du}{dy} = \dot{\gamma} = \frac{\tau}{\eta}$$

or $$\tau = \eta \dot{\gamma} \qquad \text{- - - - - - (1)}$$

Newtonian behaviour has been found to be common in all gases and liquids or solutions of low molecular weight materials.

All fluids which do not obey the law of direct proportionality of τ and $\dot{\gamma}$ in equation 1 are non-Newtonian fluids. They are further classified as:

(a) Time independent or purely viscous fluids:

Fluids for which shear rate depends only upon shear stress.

$$\dot{\gamma} = fn(\tau) \qquad \text{- - - - - - (2)}$$

(b) Time dependent fluids:

Fluids for which shear rate depends upon imposed shear stress and the duration of the stress.

$$\dot{\gamma} = fn(\tau, t) \qquad \text{- - - - - - (3)}$$

(c) Visco-Elastic fluids:

Materials for which shear rate depends upon imposed stress and extent of deformation.

$$\dot{\gamma} = fn(\tau, E) \qquad \text{- - - - - - (4)}$$

(d) Complex Rheological bodies:

Systems exhibiting the complexities of the categories a,b, and c materials in combination.

(e) Fluids for which shear rate depends upon shear stress, and intensity of an imposed magnetic field.

(f) Fluids which must be considered as being made up of discrete particles rather than as a continuous media.

Non-Newtonian behaviour is commonly observed in (i) solution or melts of high molecular weight polymeric materials, (ii) suspension of solids in liquids at sufficiently high concentration to affect or associate with the liquid phase.

Even though there are six categories of non-Newtonian fluids, virtually all engineering work to date has dealt with the first category. Also since the problem of interest in the present investigation is the one concerning this category the fluid behavior of only the Time-Independent non-Newtonians is reviewed here.

1.2.1 TIME INDEPENDENT NON-NEWTONIAN FLUIDS

The rheological equation $\dot{\gamma} = fn(\tau)$ holds for this category of fluids. They are further sub-divided into 3 distinct types depending on the plotted form of the equation. Figures 1 and 2 show the classification by the so called "flow curves".

(a) Bingham Plastic:

This is the simplest of non-Newtonian fluids and has the rheological equation

$$\tau - \tau_y = \eta_p \dot{\gamma} \qquad \text{for} \quad \tau > \tau_y \qquad \text{------ (5)}$$

where η_p = plastic viscosity or coefficient of rigidity

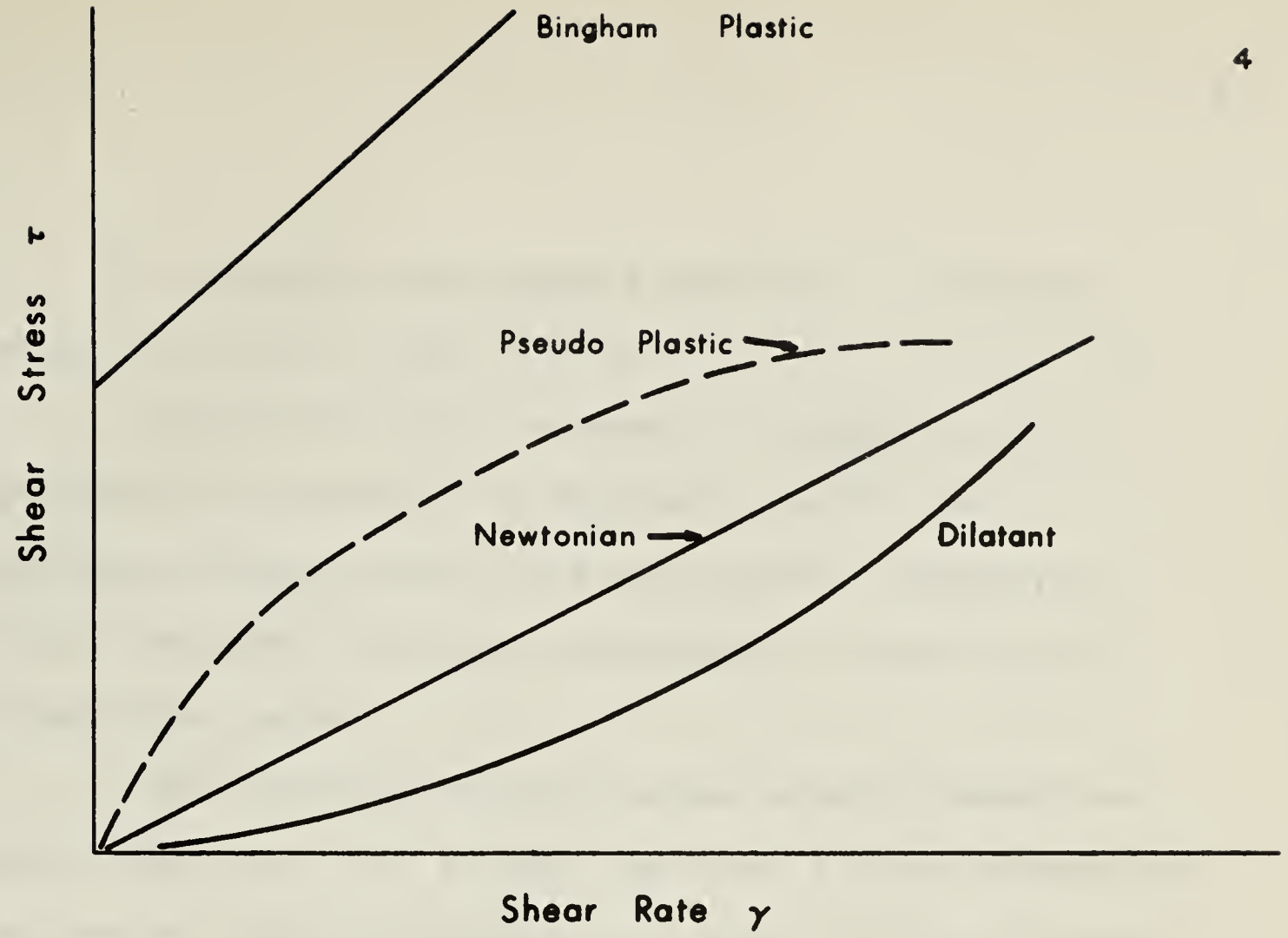

Fig. 1 Fluid Flow Curve (Arithmetic Plot)

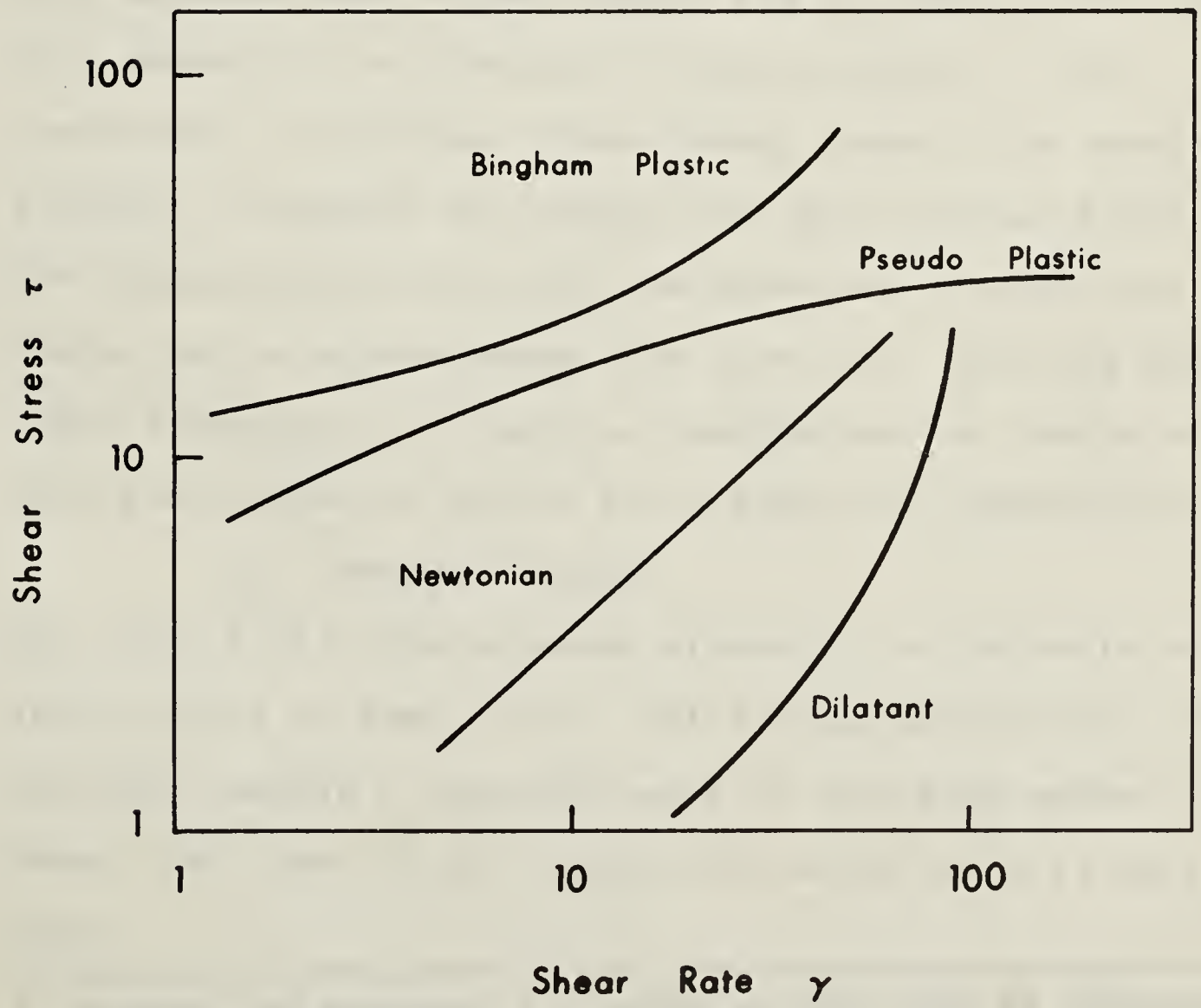

Fig. 2 Fluid Flow Curve (Logarithmic Plot)

τ_y = initial shear stress necessary to initiate movement i.e. $\dot{\gamma} = o$ for $\tau < \tau_y$

The flow curve is shown to ordinary and logarithmic co-ordinates in Figures 1 and 2. To Logarithmic Co-ordinates the curve becomes asympotitic to τ_y at low shear rates and approaches a slope of unity at high shear rates.

The explanation for Bingham plastic behaviour assumes that the fluid at rest contains a three dimensional structure of rigidity sufficiently great to resist finite stress τ_y. When the stress is exceeded the structure breaks down completely and the fluid displays the linear relationship between shear stress excess and the shear rate (1). This concept of an idealised Bingham plastic is very convenient in practice. Even though there is no convincing evidence to support the suggestion that any real fluids obey the Bingham plastic law (2) the behaviour of many real fluids can be approximated with this law. Drilling muds, chalk suspension, oil paints, toothpastes and sewage sludges have been stated to follow the Bingham law approximately (1,3).*

(b) Pseudo-Plastic:

For these fluids the "apparent viscosity" - the ratio of shear stress to shear rate - falls progressively with shear rate and reaches a limiting value at very high rates of shear. Hence, the slope of the logarithmic slope curve is less than unity.

---

* Numbers in brackets ( ) refer to the list of references.

(c) Dilatant fluids:

The apparent viscosity for these materials increases with increasing rates of shear. The slope of the logarithmic flow curve is greater than unity.

To portray the behaviour of time independent non-Newtonian fluids in general and pseudo-plastics in particular, a large number of empirical equations have been proposed. A very popular and versatile equation which predicts the behaviour approximately over a range of shear rates is the "Power Law"

$$\tau = K(\dot{\gamma})^n \qquad \text{- - - - - - (6)}$$

where K and n are constants for a particular fluid: K is generally considered as a measure of the consistency of the fluid, n is a measure of the degree of non-Newtonian behaviour. This equation with only two constants is used for pseudo-plastics ($n<1$) and also for dilatant fluids ($n>1$).

This powerlaw has three basic defects, as pointed out by Reiner (4). Since the dimensions of τ and $\dot{\gamma}$ are fixed, the term K has dimensions which depend upon the value of n. It is assumed that different materials will have different value of n, and hence K is different both qualitatively and quantitatively for different materials. Therefore K cannot be a measure of a single property such as consistency.

The apparent viscosity $\eta_a = \frac{\tau}{\dot{\gamma}} = K\dot{\gamma}^{n-1}$. Hence $\eta_a \longrightarrow \infty$ as $\dot{\gamma} \longrightarrow 0$ i.e. when fluid is at rest, and $n<1$.

This is contrary to experience as any fluid must have a definite apparent viscosity at rest; otherwise it cannot begin to flow.

Also when $n < 1$, $\eta_a \longrightarrow 0$ as $\dot{\gamma} \rightarrow \infty$ which is objectionable as there is no liquid whose viscosity vanishes.

These objections which have been discussed in detail by Reiner (4) are assumed not to be serious in most engineering applications (3) and the power law continues to be used in the same form as equation 6. The other empirical equations are more difficult to use than powerlaw and usually do not offer any compensating advantages (3).

1.3 FLOW OF NON-NEWTONIAN FLUIDS THROUGH PIPES.

The case of steady, laminar flow of a time-independent non-Newtonian fluid through a circular pipe is discussed.

Consider a fluid for which $\dot{\gamma} = f(\tau)$. For flow through circular pipes $\dot{\gamma} = -\frac{\partial u}{\partial r}$. By considering the equilibrium of a cylindrical element as shown in Figure 3.

$$2\pi r L \tau = \pi r^2 \Delta p$$

$$\tau = \frac{\Delta p}{L} \frac{r}{2}$$

At the wall

$$\tau_\omega = \frac{\Delta p}{L} \frac{R}{2}$$

$$\tau = \tau_\omega \frac{r}{R}$$

$$\therefore \quad \dot{\gamma} = -\frac{\partial u}{\partial r} = f(\tau) = f\left(\tau_\omega \frac{r}{R}\right) \text{ - - - - - - (7)}$$

Integrating, $\quad u(r) - u(R) = \int_r^R f\left(\frac{\tau_\omega}{R} r\right) dr$

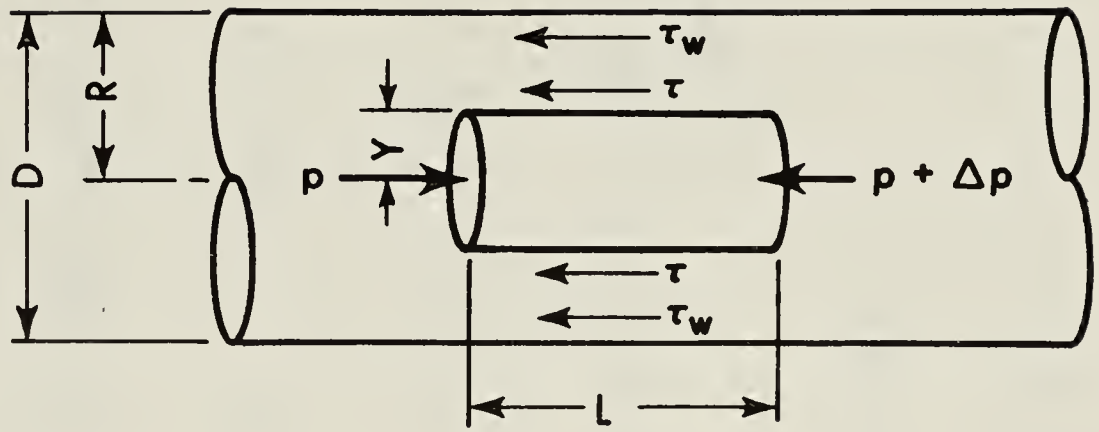

Fig. 3 Flow through a Pipe

If there is no slip at the wall $u(R) = 0$

$$\therefore \quad u(r) = \int_r^R f\left(\frac{\tau_\omega}{R}\, r\right) dr$$

Mean velocity $\quad V = \frac{1}{\pi R^2} \int_0^R 2\pi r\ u(r)\, dr$

$$= \frac{1}{R^2} \int_0^R u(r)\, d(r^2)$$

$$= \frac{1}{R^2} \left[r^2\, u(r) - \int r^2\, d\, u(r) \right]_0^R$$

But $\quad u(R) = 0$

and $\quad d\, u(r) = f\left(\tau_\omega \frac{r}{R}\right) dr \quad$ - - - from equn. (7)

$$\therefore \quad V = \frac{1}{R^2} \int r^2 f\left(\tau_\omega \frac{r}{R}\right) dr \quad \text{- - - - - - (8)}$$

Again $\quad r = R \frac{\tau}{\tau_\omega} \quad$ so that $\quad dr = \frac{R}{\tau_\omega} d\tau$

Hence inserting in equn. (8)

$$V = R \int_0^{\tau_\omega} \frac{1}{\tau_\omega^3}\, \tau^2\, f(\tau)\, d\tau$$

or $\quad \frac{8V}{D} = \frac{4}{\tau_\omega^3} \int_0^{\tau_\omega} \tau^2 f(\tau)\, d\tau \quad \text{- - - - - - (9)}$

This is the general expression for the relationship between the "flow function" $\frac{8V}{D}$ and the boundary shear for the case of steady laminar flow through circular pipes.

Knowing the form of function $f(\tau)$ the above equation can be integrated to solve for various pipe flow parameters in terms of others.

1.3.1 FOR A NEWTONIAN FLUID

$$\tau = \eta \dot{\gamma} = -\eta \frac{\partial u}{\partial r}$$

i.e. $$\dot{\gamma} = \frac{\tau}{\eta} = f(\tau)$$

From equation (9)

$$\frac{8V}{D} = \frac{4}{\tau_\omega^3} \int_0^{\tau_\omega} \frac{\tau^3}{\eta} \, d\tau$$

$$= \frac{\tau_\omega}{\eta}$$

or $$\tau_\omega = \eta \left(\frac{8V}{D}\right) \qquad \text{- - - - - - (10)}$$

But $$\tau_\omega = \frac{\Delta p}{L} \frac{D}{4}$$

$\therefore$ $$\Delta p = \frac{32 \eta V L}{D^2}$$ - - Hagen - Poiseulle equn.(10a)

Also defining the friction factor f as

$$\frac{\Delta p}{\rho g} = f \frac{L V^2}{2 g D}$$

from (10a) $$f = \frac{64}{R_e} \qquad \text{- - - - - - (11)}$$

Where $$R_e = \frac{\rho V D}{\eta}$$ = Reynolds number

The relation $\tau_w = \eta\left(\frac{8V}{D}\right)$ suggests that a plot of τ_w vs $\left(\frac{8V}{D}\right)$ can be used for testing the cases other than laminar and Newtonian since deviation from straight line in such a plot indicates a breakdown of Newtonian laminar conditions.

1.3.2 FOR A BINGHAM PLASTIC FLUID.

$$\tau - \tau_y = \eta_p \dot{\gamma} \quad \text{- - - for} \quad \tau > \tau_y \quad \text{- - equn(5)}$$

$$\dot{\gamma} = 0 \quad \text{- - - for} \quad \tau < \tau_y$$

$$\dot{\gamma} = f(\tau) = \frac{1}{\eta_p}(\tau - \tau_y) \quad \text{- - - - for } \tau > \tau_y$$

$$f(\tau) = 0 \quad \text{- - - - - - for } \tau < \tau_y$$

Equation (9) becomes

$$\frac{8V}{D} = \frac{4}{\tau_\omega^3}\left[\int_0^{\tau_y} \tau^2 f(\tau)\, d\tau + \int_{\tau_y}^{\tau_\omega} \tau^2 f(\tau)\, d\tau\right]$$

$$\frac{8V}{D} = \frac{4}{\tau_\omega^3}\int_{\tau_y}^{\tau_\omega} \tau^2 \frac{(\tau - \tau_y)}{\eta_p}\, d\tau$$

$$= \frac{4}{\eta_p \tau_\omega^3}\left[\frac{\tau_\omega^4}{4} - \frac{\tau_y \tau_\omega^3}{3} + \frac{\tau_y^4}{12}\right]$$

$$\frac{8V}{D} = \frac{\tau_\omega}{\eta_p}\left[1 - \frac{4}{3}\left(\frac{\tau_y}{\tau_\omega}\right) + \frac{1}{3}\left(\frac{\tau_y}{\tau_\omega}\right)^4\right]$$

- - - - - - (12)

This equation (12), known as the Buckingham equation, enables the relationship between pressure drop and flow rate to be determined provided the fluid properties τ_y and η_p are known. Note that it reduces to equation (10) when $\tau_y = 0$, and generalise equation (10) to allow for viscosity η being replaced by two parameters τ_y and η_p.

To solve for the pressure loss, the Buckingham equation has been expressed in non-dimensional form in a number of ways. Govier and Winning (5) divide the equation (12) by $\frac{8\rho V^2}{\eta_p}$ to introduce the friction factor in a generalised equation (11): -

$$\frac{1}{R_{em}} = \frac{f}{64} - \frac{Y}{6R_{em}} + \frac{64\,Y^4}{3f^3 R_{em}^4} \qquad \text{- - - - - - (13)}$$

where $f = \frac{\Delta p \cdot D}{L} \cdot \frac{1}{\rho V^2/2}$ = friction factor

$R_{em} = \frac{V D \rho}{\eta_p}$ = a modified Reynolds number

$Y = \frac{\tau_y D}{V \eta_p}$ = a "yield number"

Perkins and Glick (1.5) have written equation (13) as:

$$\frac{1}{R_{em}} = \frac{f}{64} - \frac{H}{6R_{em}^2} + \frac{64\,H^4}{3f^3 R_{em}^8} \qquad \text{- - - - (14)}$$

where $H = \frac{\tau_y D^2 \rho}{\eta_p^2}$ = the Hedstrom number

It will be observed that $H = Y R_{em}$. Charts are available (1,3) to give the variation of f with H (or Y) and R_{em} for the laminar region - as given by equation (12) and for the turbulent region also - as determined by experimental observations.

1.3.3 FLUIDS WHICH OBEY POWER LAW.

If $\tau = K \dot{\gamma}^n$ - - - - - - (6)

$$\dot{\gamma} = (\tau/K)^{1/n} = f(\tau)$$

From equation (9)

$$\frac{8V}{D} = \frac{4}{\tau_\omega^3} \cdot \frac{1}{K^{1/n}} \int_0^{\tau_\omega} \tau^{2+\frac{1}{n}}\, d\tau$$

$$\therefore \quad \frac{8V}{D} = \frac{4}{K^{1/n}\,\tau_\omega^3} \cdot \frac{\tau_\omega^{3+1/n}}{3+1/n}$$

i.e. $$\frac{8V}{D} = \frac{4n}{3n+1} \left(\frac{\tau_\omega}{K}\right)^{1/n} \qquad \text{- - - - (15)}$$

or $$\tau_\omega = K\left(\frac{3n+1}{4n}\right)^n \left(\frac{8V}{D}\right)^n \qquad \text{- - - - - - (16)}$$

or $$\Delta p = 4K\left(\frac{6n+2}{n}\right)^n \frac{V^n L}{D^{n+1}} \qquad \text{- - - - - - (16-a)}$$

It is interesting to observe from this equation (17) that $$\Delta p \propto \frac{V^n L}{D^{n+1}}$$

i.e. $$\Delta p \propto Q^n L / D^{3n+1}$$

i.e. For a given rate of flow in a known length of pipe the relation between the diameter of the pipe and the corresponding change in the pressure depend upon n of the fluid. Thus for pseudo-plastics ($n<1$) the pressure drop is less sensitive to diameter than for dilatant fluids ($n>1$). This fact is important in the design of capillary viscometers and metering devices for non-Newtonian fluids.

The equation (6) together with equation (15) can be used as follows to get an expression for $\left(-\frac{\partial u}{\partial r}\right)$ i.e. the shear rate at any radial distance r:

$$\dot{\gamma} = -\frac{\partial u}{\partial r} = \left(\frac{\tau}{K}\right)^{1/n} \qquad \text{- - - from equn (6)}$$

but $$\tau = \tau_\omega \left(\frac{r}{R}\right)$$

$$\therefore \; -\frac{\partial u}{\partial r} = \left(\frac{\tau_\omega}{K}\right)^{\frac{1}{n}} \left(\frac{r}{R}\right)^{1/n}$$

Using equation (15), $$\left(-\frac{\partial u}{\partial r}\right) = \frac{3n+1}{4n}\left(\frac{8V}{D}\right)\left(\frac{r}{R}\right)^{1/n} \qquad \text{- - (17)}$$

1.3.4 ANY TIME INDEPENDENT NON-NEWTONIAN FLUID.

$$\frac{8V}{D} = \frac{4}{\tau_\omega^3}\int_0^{\tau_\omega} \tau^2 f(\tau)\, d\tau \qquad \text{- - - - - - (18)}$$

$\therefore \frac{8V}{D}$ is a function of τ_ω, say $\phi(\tau_\omega)$

$$\therefore \; \phi(\tau_\omega) = \frac{4}{\tau_\omega^3}\int_0^{\tau_\omega} \tau^2 f(\tau)\, d\tau$$

or $$f(\tau_\omega) = \frac{1}{4\tau_\omega^2} \cdot \frac{d\left[\tau_\omega^3 \phi(\tau_\omega)\right]}{d\tau_\omega}$$

$$\text{i.e. } f(\tau_\omega) = \frac{1}{4\tau_\omega^2}\left[\phi(\tau_\omega)\cdot 3\tau_\omega^2 + \tau_\omega^3\, d\phi(\tau_\omega)\right]$$

$$= \frac{3}{4}\phi(\tau_\omega) + \frac{\tau_\omega}{4}\frac{d\phi(\tau_\omega)}{d\tau_\omega}$$

But $$f(\tau_\omega) = \dot{\gamma}_\omega = \left(-\frac{\partial u}{\partial r}\right)_\omega$$

$$\therefore \quad \left(-\frac{\partial u}{\partial r}\right)_\omega = \frac{3}{4}\left(\frac{8V}{D}\right) + \frac{\tau_\omega}{4}\frac{d\left(\frac{8V}{D}\right)}{d\tau_\omega} \qquad \text{- - - - (19)}$$

This equation which gives the shear rate at the wall for any time independent non-Newtonian is known as the Robinowitsch - Mooney equation. The solution as above was first given by Mooney (6,1).

Metzner and Reed (7) have made the following useful alteration of the above equation (19) using the identity $\frac{\tau_\omega}{4}\frac{d\left(\frac{8V}{D}\right)}{d\tau_\omega} = \frac{\left(\frac{8V}{D}\right)}{4}\cdot\frac{d\left(\text{Log }\frac{8V}{D}\right)}{d\,\text{Log }\tau_\omega}$:-

$$\left(-\frac{\partial u}{\partial r}\right)_\omega = \frac{3}{4}\left(\frac{8V}{D}\right) + \frac{1}{4}\left(\frac{8V}{D}\right)\frac{d\left(\log\frac{8V}{D}\right)}{d\log\tau_\omega}$$

Let $$\frac{d\left(\log\frac{8V}{D}\right)}{d\log\tau_\omega} = \frac{1}{n'} \qquad \text{- - - - - - (20)}$$

that is n^1 is the slope at any point of the curve $\log\tau_\omega$ vs $\log\left(\frac{8V}{D}\right)$,

Then $$\left(-\frac{\partial u}{\partial r}\right)_\omega = \left(\frac{3n'+1}{4n'}\right)\left(\frac{8V}{D}\right) \qquad \text{- - - - - - (21)}$$

Also from equation (20), $\log\tau_\omega = n^1 \log\left(\frac{8V}{D}\right) + \text{Log } K^1$

$$\therefore \quad \tau_\omega = K'\left(\frac{8V}{D}\right)^{n'} \qquad \text{- - - - - - (22)}$$

Equations (21) and (22) should hold good for any time independent fluid regardless of the shear rate - shear stress relationship, provided there is no slip at the wall. Thus, even though the shear stress and shear rate vary from point to point inside a tube, the relation between τ_ω and $\frac{8v}{D}$ is unique for laminar flow of any time independent fluid. This relationship, which may be conveniently determined in a capillary-tube viscometer defines the characteristic behaviour of a fluid just as completely as shear rate - shear stress relationship.

In general n' and K' may be expected to vary for a fluid. However, if n' and K' are constant - i.e., if the logarithmic plot of τ_ω and $\frac{8v}{D}$ is a straight line - the equation (22) becomes the power law for a fluid (equation 16). Then $n' = n$

$$\text{and} \quad K' = K \left(\frac{3n+1}{4n}\right)^n \qquad \text{- - - - - - - (22a)}$$

It is interesting to note that the unique correlation between τ_ω and $\frac{8v}{D}$ is applicable only for laminar flow. Outside the laminar flow region the relation - ship between τ_ω and $\frac{8v}{D}$ is dependent on the pipe diameter (8,9)

Equation (22) can be re-arranged as below to define the friction factor **f** for laminar flow:

$$f = \frac{\Delta p}{L} \frac{D}{\rho V^2/2}$$

$$= \frac{8}{\rho V^2} \tau_\omega$$

$$= \frac{8}{\rho V^2} K' \left(\frac{8V}{D}\right)^{n'}$$

$$= \frac{64\, K' (8)^{n'-1}}{\rho V^{2-n'} D^{n'}}$$

$$\therefore \quad f = \frac{64}{R'_e} \qquad \text{- - - - - - (23)}$$

$$\text{where } R'_e = \frac{\rho V^{2-n'} D^{n'}}{K' (8)^{n'-1}}$$

Comparing equation 23 with the corresponding equation for Newtonian flow viz

$$f = \frac{64}{Re} \qquad \text{- - - - - - (equn. 11)}$$

Metzner (10, 1,2) calls R'_e a generalised Reynolds number. It enables the data for both Newtonian and non-Newtonian fluids to be represented in non-dimensional form in a plot of f vs R'_e. For laminar flow the relation between f and R'_e from equation (23) would be a straight line in a logarithmic plot. Metzner and Dodge (10) have extended the idea of the generalised Reynolds number to obtain f vs R'_e relation for turbulent flow also as in Fig. 4.

1.4.1 ANOMALOUS FLOW NEAR A WALL.

In the derivation of the equation 9 it was assumed that there was no "slip" at the wall. However in certain non-Newtonian fluids (eg. certain high polymer materials and certain suspensions) the presence of a boundary introduces a preferred orientation of molecules or particles near the wall in an otherwise isotropic material. In the case of suspension of solids sometimes a thin film of lower consistency may form near the boundary and give rise to an "effective slip velocity" at the wall.

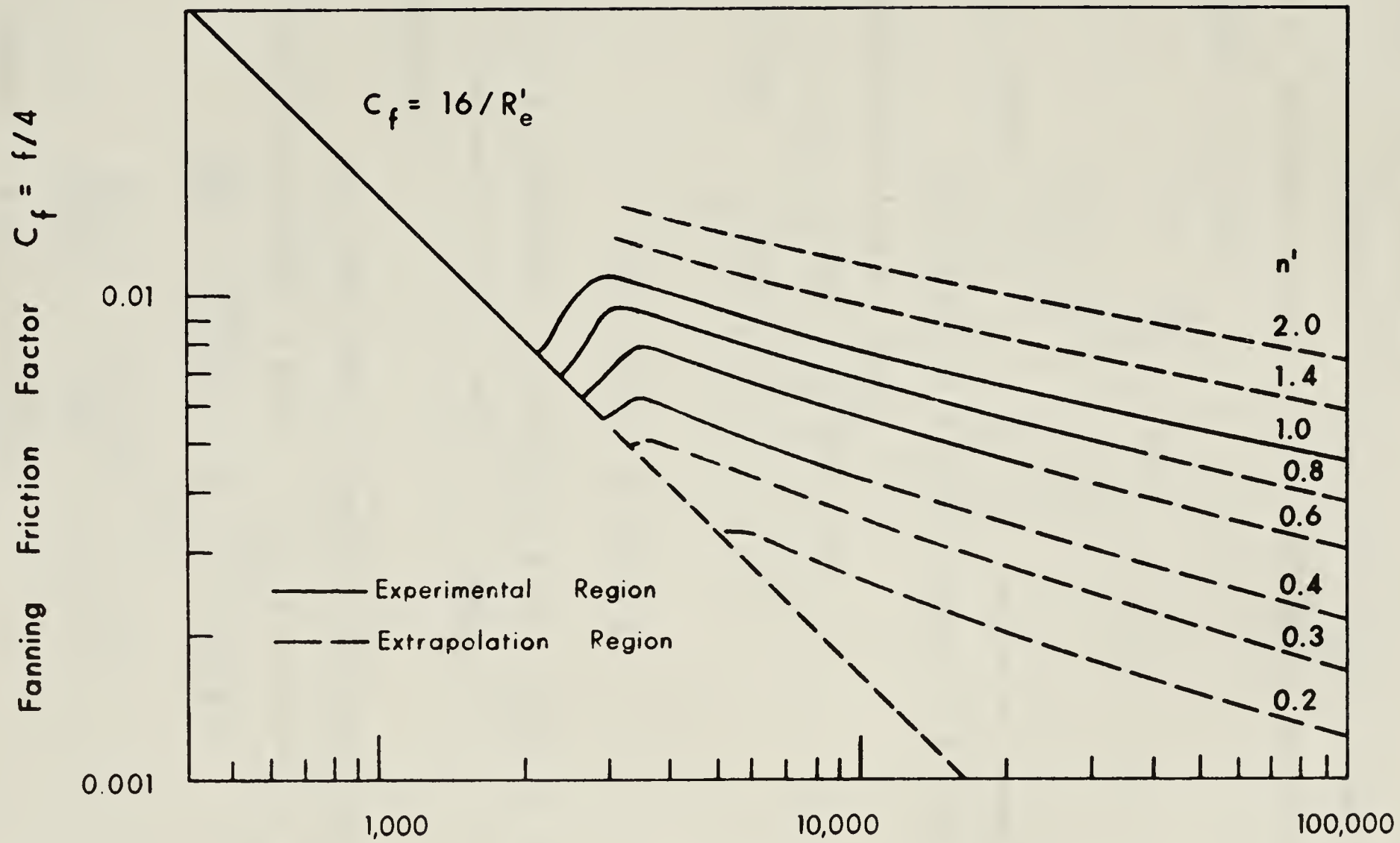

Fig. 4 Friction factor - Reynolds Number Design Chart for Purely Viscous Fluids (Ref. 10)

Oldroyd (11) calculates the "effective slip velocity" as follows:

Assume that in a small region close to the wall, i.e. within a range $0<y<\epsilon$, the shear rate will differ from $\dot{\gamma} = f(\tau)$.

i.e. $$\frac{du}{dy} = f(\tau) + g(\tau, y) \qquad \text{- - - - - - (24)}$$

Where $g(\tau,y) = 0$ when $y > \epsilon$.

The region $0<y<\epsilon$ is called the region of anomalous flow.

The velocity u just outside the region of anomalous flow is then

$$u = f(\tau)y + \int_0^{\epsilon} g(\tau,y)\, dy \qquad \text{- - - - - - (25)}$$

;writing $$\int_0^{\epsilon} g(\tau,y)\, dy \equiv s(\tau)$$

$$u - s(\tau) = f(\tau)\, y \qquad \text{- - - - - - (26)}$$

$S(\tau)$ is therefore the value of u at y=o and is the effective slip velocity at the wall. It depends upon the local shear stress τ.

For the case of laminar flow through a round tube, substituting $u(R) = s(\tau_\omega)$ in the derivation of equation (9)

$$\frac{8V}{D} = \frac{4\, s(\tau_\omega)}{R} + \frac{4}{\tau_\omega^3} \int_0^{\tau_\omega} \tau^2 f(\tau)\, d\tau \qquad \text{- - - - - (27)}$$

$$\frac{8V}{D\tau_\omega} = \frac{4\, S(\tau_\omega)}{R} + \psi(\tau_\omega) \qquad \text{- - - - - (28)}$$

Where $$S(\tau_\omega) = \frac{s(\tau_\omega)}{\tau_\omega}$$

$$\psi(\tau_\omega) = \frac{4}{\tau_\omega^4} \int_0^{\tau_\omega} \tau^2 f(\tau)\, d\tau$$

$S(\tau_\omega)$ is called, by Oldroyd (11), the effective slip coefficient and is the effective velocity of slip per unit shear stress at the wall.

Equation (28) can be solved, in principle, for $S(\tau)$ and $f(\tau)$, by **making** observations on different diameter tubes. If there is any anomalous behaviour the plots of $\frac{8V}{D} \cdot \frac{1}{\tau_\omega}$ vs τ_ω will be dependent on the value of D.

However, it must be remembered, that $\frac{8V}{D\tau_\omega}$ vs τ_ω curves will be dependent on D at high values of τ_ω due to onset of turbulence. This should not be misinterpreted as wall effect.

1.4.2 **PARTICLE** SLIP VELOCITY IN VERTICAL PIPES.

For steady flow of suspensions in vertical pipes Kada and Henratty (23) observe that even though the concentration at a section be constant with respect to time the average velocity of the particles could be different from that of the fluid. The difference between the average velocity of the particles and the average velocity of the fluid is called "the particle slip velocity". The free fall velocity of the particles is a close approximation to the "particle slip velocity" (23) if the concentration of the suspension is not appreciable.

This "particle slip velocity" which is different from the "effective slip velocity" of Oldroyd, is important in the capillary viscometer studies. If the volume concentration of solids is determined from the quantity of

suspension discharged from the capillary tube in a known interval of time, the observed concentration will tend to be greater than the actual concentration.

CHAPTER II

FLOW BEHAVIOUR OF SUSPENSIONS

2.1 A suspension being a system of solid particles dispersed in a liquid medium one can visualise many types depending on the physical characteristics of the solid and the liquid phases. However, only those suspensions will be considered in which the liquid is Newtonian and the solids are rigid, do not react with the liquid and do not possess electrical charge.

Generally one can expect the "apparent viscosity" η_a of such a suspension - defined as the ratio of shear stress to shear rate at a specified shear rate - to depend on:

(1) the concentration of solids

(2) the shape, size, and mass of the solid particles

(3) the viscosity and density of the suspending medium

(4) the shear rate

Frisch and Simha (12) consider the suspension in three concentration regions wherein a characteristic behaviour is present, viz,

(a) extremely dilute suspensions

(b) dilute suspensions

(c) concentrated suspensions

Taking these in detail:

2.1.1 EXTREMELY DILUTE SUSPENSIONS

In these the suspension is so dilute that the distances between the particles are effectively infinitely

great in comparison to their sizes. During motion, every particle produces a disturbance in an otherwise laminar flow around it in a restricted field. The disturbances due to two adjacent particles do not overlap.

Einstein, in 1905, found a mathematical solution for the case of rigid spheres in a Newtonian liquid, under the assumption of extreme dilution (4) as

$$\eta_r = 1 + 2.5\ C \qquad \text{- - - - - - (29)}$$

where η_r = relative viscosity

$$= \frac{\text{Apparent viscosity of the suspension}}{\text{Viscosity of the suspending medium}}$$

C = Volume concentration

$$= \frac{\text{Volume of solids}}{\text{Volume of the suspension}}$$

Equation 29 indicates that the suspension behaves as Newtonian liquid in this region of extreme dilution, as η_r is independent of the shear rate. Einstein's equation has been found to be valid for values of concentrations up to about 3 percent (4).

Following Einstein's approach many theoretical studies have been conducted on infinitely dilute suspensions of solid particles of various shape (12) and the result can be generally expressed as

$$\eta_r = 1 + a_1 C \qquad \text{- - - - - - (30)}$$

where

a_1 is a function of dimensionless geometric

parameters characterising the shape of the particle.

It is interesting to note that the densities of the solid and liquid components of the suspension do not have any effect on the consistency of the suspension in this range.

Thus the infinitely dilute suspension - or real suspension with volume concentration less than 3 percent - behaves like a Newtonian fluid and the relative viscosity is a linear function of the concentration.

2.1.2 DILUTE SUSPENSIONS.

In these suspensions the disturbances produced by the adjacent particles interact. The dependence of viscosity on concentration is no more linear. Numerous theoretical and empirical solutions have been proposed by assuming various models to represent the interaction. A good review of works in this range is given by Frisch and Simha (12). Generally the concentration dependence of viscosity is expressed as a polynomial with the values of coefficients depending on the shape of the particles. However the effect of shear rate is not considered in any of the work reviewed in ref. (12).

2.1.3 CONCENTRATED SUSPENSIONS.

In these the particles will be so close together that they form networks, with flow immobilising power far

greater than that in the dilute suspensions. This regime corresponds to a concentration in which particles may form close packing. Frisch and Simha (12) observe that non-Newtonian behaviour is to be expected in a real suspension in this range. A review of the theoretical works in this field given in ref.(12)indicate that the formulas derived from the theoretical approach have not considered the effect of shear rate.

Thus the theoretical and semi theoretical approaches to the problem of viscosity of dilute and concentrated suspensions have all assumed Newtonian behaviour and other simplifying pictures of particle interaction. The result is a host of fomulae, which can be described as confusing, to say the least, when it comes to the application to a specific case. This has been demonstrated in a dramatic way in a review by Rutgers (16).

2.1.4 Rutgers (16) has reviewed 280 references in the field of colloidal physics and rheology, and 96 formulas proposed for the effect of concentration on the relative viscosity of a suspension of rigid spheres. All these 96 formulae purport to give η_r-C relations for the Newtonian range. Other than Einstein's formulas (equation 29), which is valid up to C= 0.03, Rutgers found that only 5 of the remaining formulas have validity over the whole concentration range. Also only two of these five

formulae are easy to handle and are based on some theoretical argument. They are

Mooney's equation:

$$\text{Ln}\ \eta_r = \frac{KC}{1-SC} \qquad \text{- - - - - - (31)}$$

where

$K = 2.76$	or	$K = 2.50$
$S = 1.29$		$S = 1.40$

η_r = relative viscosity

Vand's equation:

$$\frac{1}{\eta_r} = (1 - A_1 C + A_2 C^2)^n \qquad \text{- - - - - - (32)}$$

where

$A_1 = 1.10$	or	$A_1 = 1.00$
$A_2 = 0.97$		$A_2 = 1.20$
$n = 2.50$		$n = 2.50$

These formulas were derived for suspensions of rigid spheres in Newtonian liquid. The specific gravity of the solids was the same as that of the liquid. Also the suspensions were assumed to behave as Newtonian fluids - presumably at very low shear rates.

In another paper Rutgers (17) has reviewed 21 investigations on the suspension of rigid spheres in Newtonian liquid. The spheres were of the same specific gravity as the liquid and of sizes 0.3 to 400 microns. The distribution of any one grain size was such as to include a moderate amount of grains of adjacent sizes. Rutgers (17) observes that the investigations reviewed by him seem to indicate that the suspensions of the above type behave as Newtonian up to C = 0.25.

Also he indicates that there seem to be several volume concentrations where the flow behaviour shows changes e.g. at C = 0.02 - 0.15 - 0.20 - 0.25 - 0.45 - C max.

However, a study of the data used by Rutgers (17) shows that most of the experiments were conducted either at constant values of τ or $\dot{\gamma}$ or the range of shear rate used was very small. The maximum shear rate used in any experiment was 1860 sec^{-1}. With this in view much weight cannot be attached to the conclusion that Newtonian behaviour occurs up to C = 0.25 in all suspensions.

From these reviews (12,16,17) one can conclude that inspite of the numerous works that has been done on this topic in the field of colloidal science and rheology, there is no full appreciation of the various factors affecting the behaviour of suspensions. This is especially so with regard to non-Newtonian behaviour.

2.2 NON-NEWTONIAN BEHAVIOUR OF SUSPENSIONS.

The earliest study on dilatant behaviour was by Osborne Reynolds. His original explanation given in 1888 is probably the best explanation for dilatancy. (1). "He assumed that suspensions of solids at high concentrations when at rest consist of densely packed particles in which the percent of voids is small and perhaps minimum. Sufficient liquid is present only to fill the voids. The motion of shear of such fluids at low shear rates

requires only small shearing stresses since the liquid lubricates the passage of one particle past another. At increasing rates of shear the dense packing of the solids is progressively broken up and since there was only minimum of voids the liquid present is insufficient to fill the voids and lubricate them. This causes the shear stress to increase more than proportionately with the shear rate." This explanation suggests that all suspensions of solids in liquids should exhibit dilatant behaviour at high solid contents (1).

Freundlich and Roder working with starch-water and quartz-water systems found that an increase in the viscosity of the system sometimes occurs with increases in the shear rate (13). This was also termed dilatant behaviour as it was similar to the dilatancy described by Reynolds, even though the mechanism may have been different. Thus the term "dilatant" has since been used for all fluids which exhibit the property of increasing apparent viscosity with increasing rates of shear. Metzner and Whitlock (13) have found that volumetric dilation (as in Reynolds theory) may occur quite separately from dilatancy in the rheological sense.

In the Chemical Engineering field the non-Newtonian behaviour of suspensions has long been recognized. Thomas (18) has completely investigated the behaviour of Thorium oxide and other materials of particle size 0.35 - 13 microns by assuming the Bingham plastic law. However,

regarding the suspensions of sand size particles which exhibit dilatant behaviour, there is no similar work which has tried to unify the effects of various factors - concentration, particle size etc.- on the consistency in the non-Newtonian range.

Various investigators have tried to determine the onset of dilatancy in suspensions and their result is summarized in the following Table No. 1 taken from ref. (13).

TABLE 1

SUMMARY OF TESTS ON DILATANCY

INVESTIGATOR	SOLIDS	LIQUID VISCOSITY CENTIPOISE	PARTICLE SIZE (MICRONS)	DILATANCY OBSERVED AT CONCN.	MAX. SHEAR RATE SEC
METZNER	TiO_2	1,7,42	0.2-1.0	30 - 47	1000
	Glass beads	18,42	24 - 32	possibly 64	1300
		42	53 - 62	"	1300
		42	85 - 105	none	700
		42	24 - 105	none	1300
FREUNDLICH & RODER	Quartz	1	1 - 5	42 - 45	-
	Glass beads	154,241	3,4	none	639
		136,234	4,10	none	639
		71,94	10,30	none	639
VAND	Glass beads	80	100-160	none	about 100

The Table 1 indicates that the search is for a unique concentration at which the flow changes from Newtonian to dilatant behaviour irrespective of the other properties of the solid and liquid phase. It is the contention of the author that there is no apriori reason to assume such a unique concentration. The beginning of dilatant behaviour must be functionally related to the liquid, solid, and the flow properties of the system viz., density and viscosity of the liquid, concentration, size, shape and density of the particle and the shear rate and its variation in the system. Only by dimensional analysis and operation of dimensionless terms can it be hoped to determine the transition zone uniquely - in terms of the other variables.

2.3 BAGNOLD'S APPROACH

Bagnold (19,20) has introduced a new concept for the analysis of flow of solids in suspension. Considering a simplified model of an array of solid spheres he has shown, as outlined below, that as a result of momentum transfer between successive layers of the suspension, a repulsive pressure P_s between the grains and a shear stress τ_s should exist. This shear stress τ_s is additional to any residual stress τ_f due to momentum transfer within the intergranular fluid. i.e., it will be additional to that necessary for the motion of the fluid only.

Suppose a mass of rigid elastic spheres with uniform diameter is arranged in a tetrahedral - rectangular pattern which gives a minimum void space (corresponding to volume concentration C*). Let it be uniformly dispersed so that distance d between the centres is increased to bd (Fig. 5).

The free distance between two adjacent spheres is a.

Then $bd = a+d$

or $b = \frac{a}{d} + 1 = \frac{1}{\lambda} + 1$

where $\lambda = \frac{d}{a}$ = "Linear concentration"

$$= \frac{1}{\left(\frac{C_*}{C}\right)^{1/3} - 1} \qquad \text{- - - - - - (33)}$$

- - - (Proof in App. B)

where C* = Maximum possible value of C when all grains are in static contact.

C* = 0.74 for perfect spheres

= 0.65 for natural uniformly rounded grains (20)

Bagnold assumes that:

(a) there is no slip between the solids and the liquid

(b) a steady uniform velocity gradient $\frac{du}{dy}$ **prevails throughout the mixture**

(c) kinetic energy per unit volume is maintained constant by frictional losses

(d) in addition to average velocity U, the motion of each sphere consists of three-dimensional oscillations caused by succession of elastic collisions between spheres in faster and slower moving layers

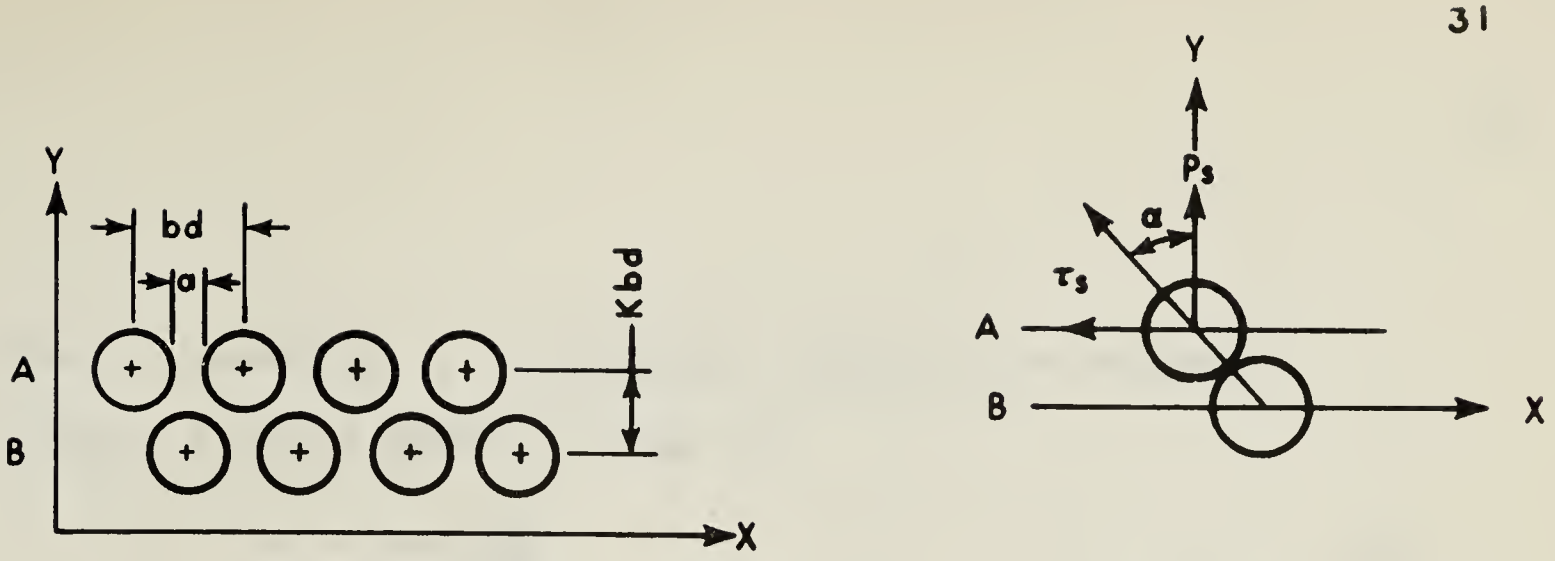

Fig. 5 Definition Sketch

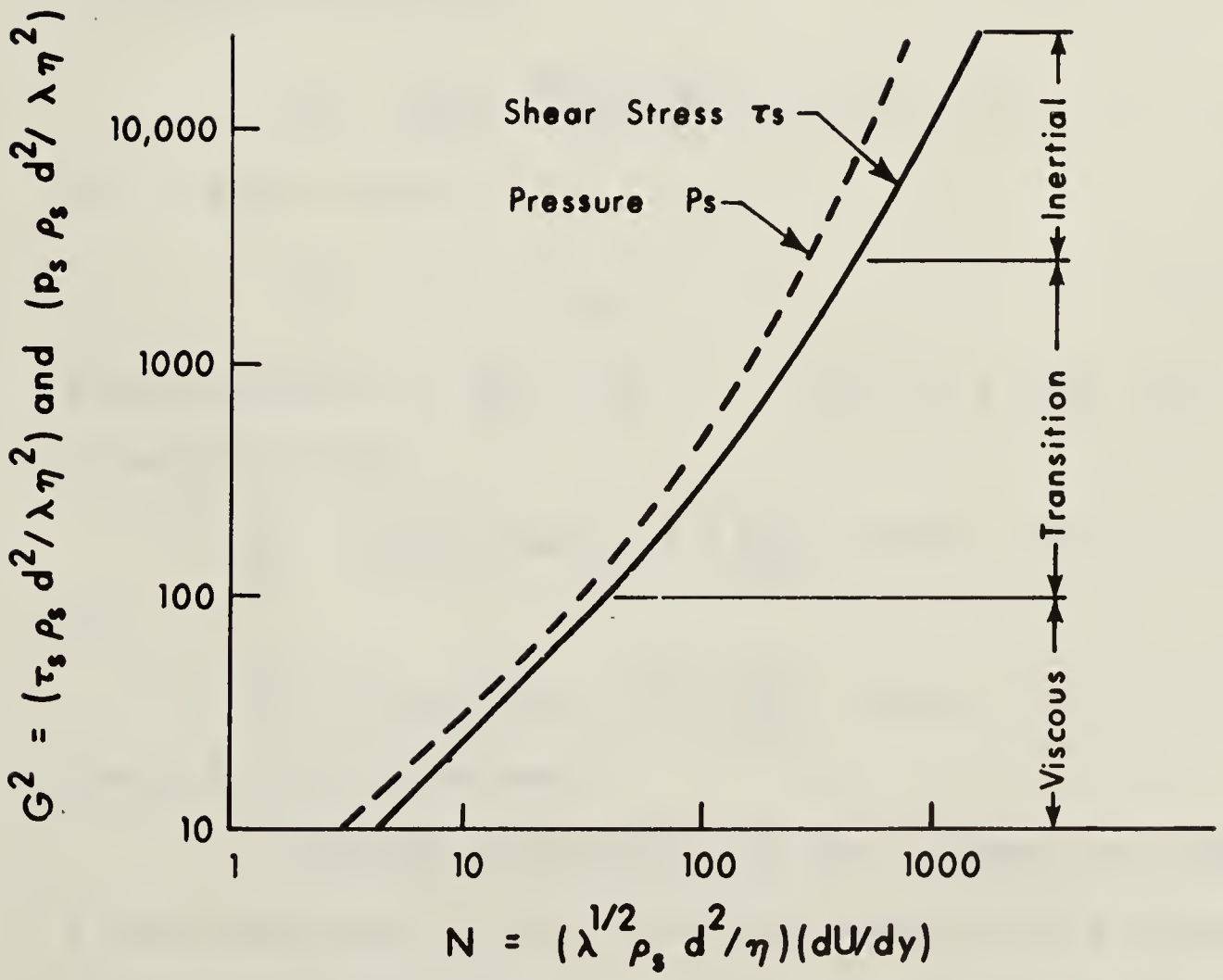

Fig. 6 Correlation between G^2 and N (Ref. 19)

Then, according to Bagnold, between two adjacent layers A and B shown in Fig. 5,

$$\delta U = Kbd \frac{du}{dy} \qquad \text{- - - - - - (64)}$$

where K is a constant. Consider the motion of grains A relative to grains B. Let the number of collisions made in $\frac{a}{\delta U}$ seconds be a function of λ i.e., $\frac{Fn\,(\lambda)\,\delta U}{a}$ collisions occur in unit time. The number of grains in unit area in each layer is $\frac{1}{(bd)^2}$. Each grain in A collides at some angle α with the grains B, thereby experiencing a total change of momentum $2m\,\delta U\,Cos\alpha$ in the y direction and $2m\,\delta U\,Sin\alpha$ in x direction, (m = mass of sphere). This gives rise to a repulsive pressure

$$p_s = \frac{1}{b^2 d^2} \frac{Fn(\lambda)\,\delta U}{a} 2m\,\delta U\,Cos\alpha \qquad \text{- - - - - (35)}$$

and a shear stress

$$\tau_s = p_s \tan\alpha \qquad \text{- - - - - - (36)}$$

Substituting $m = \frac{\pi}{6} d^3 \rho_s$ and for a and δU in equation 35,

$$p_s = K_1 \rho_s \lambda\, Fn(\lambda)\, d^2 \left(\frac{du}{dy}\right) \cos\alpha \qquad \text{- - - - - - (37)}$$

and

$$\tau_s = K_1 \rho_s \lambda\, Fn(\lambda)\, d^2 \left(\frac{du}{dy}\right) \sin\alpha \qquad \text{- - - - - - (38)}$$

Where K_1 is a constant.

Bagnold distinguishes two regimes of flow; Inertial (Corresponding to high rates of shear) and Viscous (Corresponding to low shear rates). The theory as above is for the inertial range. For the viscous range in which

fluid viscosity predominates, Bagnold gives a similar theory (19) with the relation between shear rate and shear stress given by:

$$\tau_t = \eta(1+\lambda)(1+f'(\lambda))\frac{du}{dy} \qquad \text{- - - - - - (39)}$$

Where τ_t = **total shear stress due to the effect of fluid viscosity as modified by the presence of grains**

Bagnold conducted experiments in a rotary viscometer with spherical grains of diameter 0.13 cm. and density the same as that of the suspending medium. The shear stress necessary to prevent the movement of the inner cylinder and the dispersive pressure on the inner wall were measured. It was found that both τ_s and p_s when expressed as dimensionless groups

$$G_T^2 = \frac{\tau_s \rho_s d^2}{\lambda \eta^2}$$

and

$$G_p^2 = \frac{p_s \rho_s d^2}{\lambda \eta^2}$$

bear a single valued empirical correlation with the dimensionless group

$$N = \lambda^{\frac{1}{2}} \rho_s d^2 \left(\frac{du}{dy}\right)\Big/\eta$$

This correlation between G^2 and N obtained by Bagnold is shown in Fig. 6. This relation gives

$$\tau_s = 0.013\, \rho_s (\lambda d)^2 \left(\frac{du}{dy}\right)^2$$

for inertial region - - - - - - (40)

$$\tau_s = 2.25\ \lambda^{3/2}\ \eta\ \frac{du}{dy}$$

for viscous region - - - - - - - (40a)

The transition from viscous to inertial region is between $G^2 = 100$ to 3000.

It will be noticed that

$$G_T^2 = \frac{\tau_s \rho_s d^2}{\lambda \eta^2}$$

$$\therefore \quad G_T = \frac{d.(\tau_s/\lambda\rho_s)}{\eta/\rho_s}$$

which is of the same form as :

$$\frac{d.(\tau/\rho)}{\eta/\rho}$$

$$= \frac{d\,u_*}{\nu}$$

$= R_{e*}$

= shear Reynolds number used in problems connected with sediment transportation in open channels.

2.4 CRITICAL CONCENTRATION.

In the rheological behaviour of suspensions there seems to be a critical concentration at which there is a sudden change in the apparent viscosity. Frisch and Simha (12) have indicated that at concentrations near close packing one might expect strong and abrupt increase in the apparent viscosity of the suspension. Schack et al (14) have reported the occurrence of a critical concentration at which the apparent viscosity rapidly rises with a small rise in the concentration.

This critical concentration was at C = 0.50 for quartz, feldspar, glass and calcite of sizes 5-50 microns. For gypsum C_{cr} was at 0.45 and for mica it was 0.35. Moreland's (15) experiments of suspensions of coal (80-250 mesh size) in mineral oil indicate that at C=0.30 the apparent viscosity starts increasing at a very rapid rate with the concentration. Rutgers (7) mentions several critical concentrations at which the flow behaviour may change. It is interesting to note that "for spheres at C=0.25 rotation of the spheres may begin to be hindered and C=0.45 interlocking will start" (7).

Thus, it seems, depending upon the shape of the particle, there exists a critical concentration at which an abrupt change occurs in the rheological behaviour. Also one may expect this critical concentration to have values between 0.30 and 0.50.

CHAPTER III

EXPERIMENTAL INVESTIGATION.

3.1 INTRODUCTION

A special investigation of the rheological behaviour of sand-water suspensions was undertaken in the Hydraulic Laboratories of the University of Alberta.

The justifications for the investigations were:

(1) The inadequacy of previous work (sec. 2.1 and 2.2)

(2) The need to understand the simpler aspects of concentrated sand transport in water as a preliminary to explaining the nature of transport in the saltating cloud in the duned sand bed of a canal or a river. This later unsolved problem has assumed new importance in the International Hydrologic Decade.

(3) Possible relation of the results to means for estimating transport in pipes from flow parameters.

The aims of the investigations were:

(a) To develop a viscometer for the rapid and yet accurate determination of the rheological properties of the suspensions.

(b) To obtain data on sand-water suspensions from the above viscometer and analyze them in the light of present knowledge of the flow of non-Newtonian fluids and the behaviour of suspensions.

(c) To study the applicability of Bagnold's hypothesis to laminar flow through vertical pipes.

3.2 CAPILLARY VISCOMETER.

Many instruments considered as multi-speed or multi pressure viscometers are available commercially, but most are rotating concentric cylinders, rotating discs, or cone and plate type. They are usually restricted in designed working range which cannot be altered easily. Also a good rotating viscometer to cover a wide range of shear values with reasonable accuracy is quite expensive. From the consideration of these points it was decided that a capillary viscometer be designed and built to cater to the special needs of testing of sand suspensions. This has a special advantage that the information obtained from such an instrument can be directly related to flow through pipes under appropriate conditions.

The essential features of a capillary viscometer are:

(a) A Storage Chamber. This should have an agitation mechanism for preparation of suspensions.

(b) Device for precise control and measurement of pressure.

(c) A Capillary tube.

(d) Discharge measuring device.

(e) Temperature Control.

There are different capillary viscometers, with different modifications to suit the particular needs of the problem, mentioned in the literature on viscometry (1, 21, 22, 14). Noting the advantages and disadvantages of many of these, and with the object of developing a simple, convenient, rapid

and yet sufficiently accurate instrument the following final design of a capillary viscometer was built after many trials.

Fig. 7, 8, shows the schematic diagram of the viscometer setup. Figures 9 to 13 show the various details.

3.2.1 STORAGE CHAMBER

A Chamber of capacity 500 c.c. was made by using a standard plastic pipe 3" O.D, 5 5/8" long, and connecting the two ends to brass plates by water tight seals as shown in Fig. 9. A concentric 3½" O.D. plastic pipe provided the water jacket. An agitator mechanism consisting of two sets of blades mounted on a pair of brass shafts was powered by a 1/30 H.P., 1,550 r.p.m. motor through a chain drive.

3.2.2 PRESSURE REGULATIONS.

The mixing chamber was connected to the pressurized air supply through a 0-30 p.s.i. fine control pressure regulator. The pressure in the chamber was measured by a manometer. Bromoform (sp. gr. 2.87) or mercury was used as manometer liquid depending of the order of pressure to be measured.

3.2.3 CAPILLARY TUBE.

The capillary tube for use in this instrument was formed as a separate attachment. Two sizes of capillaries

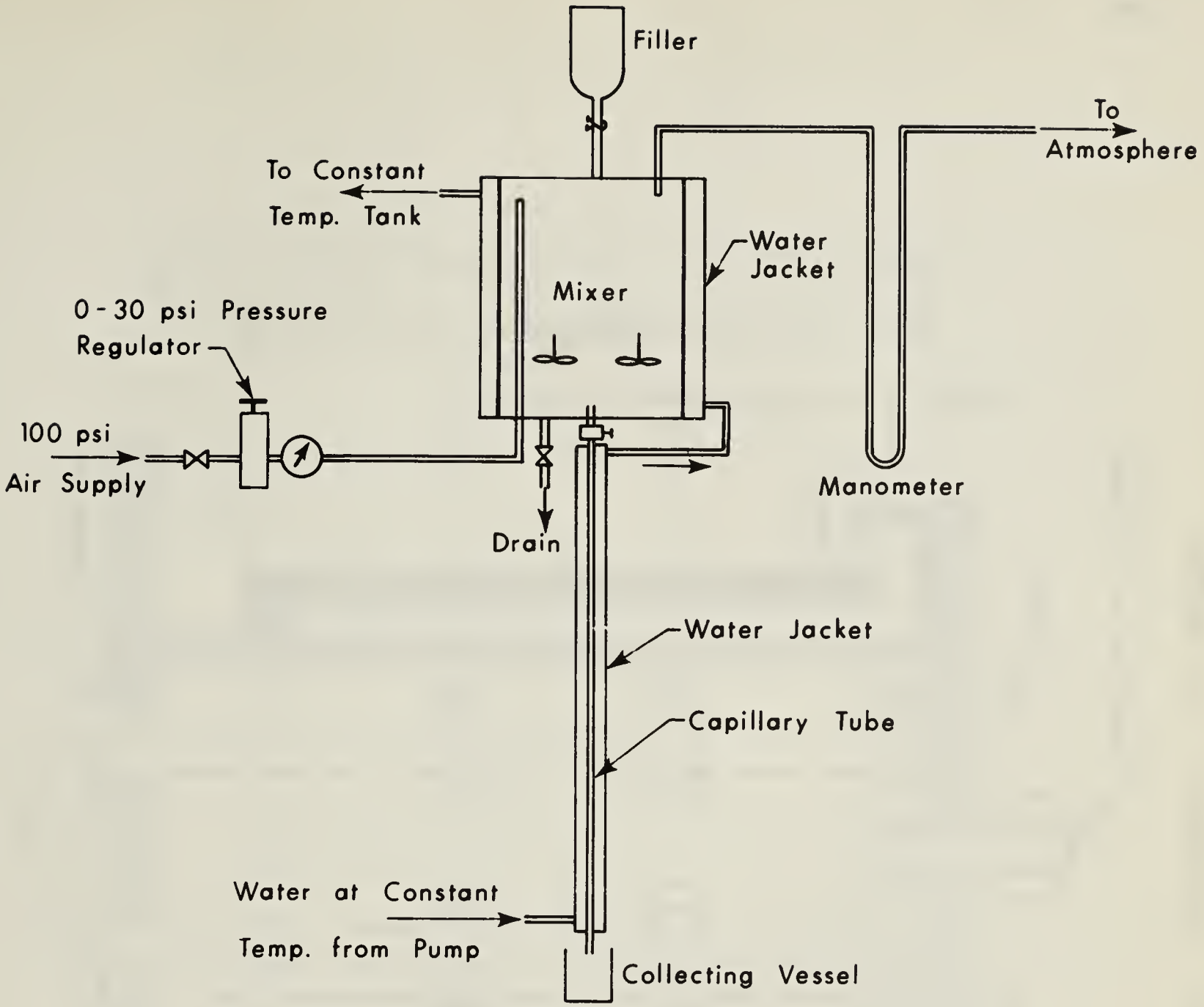

Fig. 7 Schematic Diagram of Capillary Viscometer

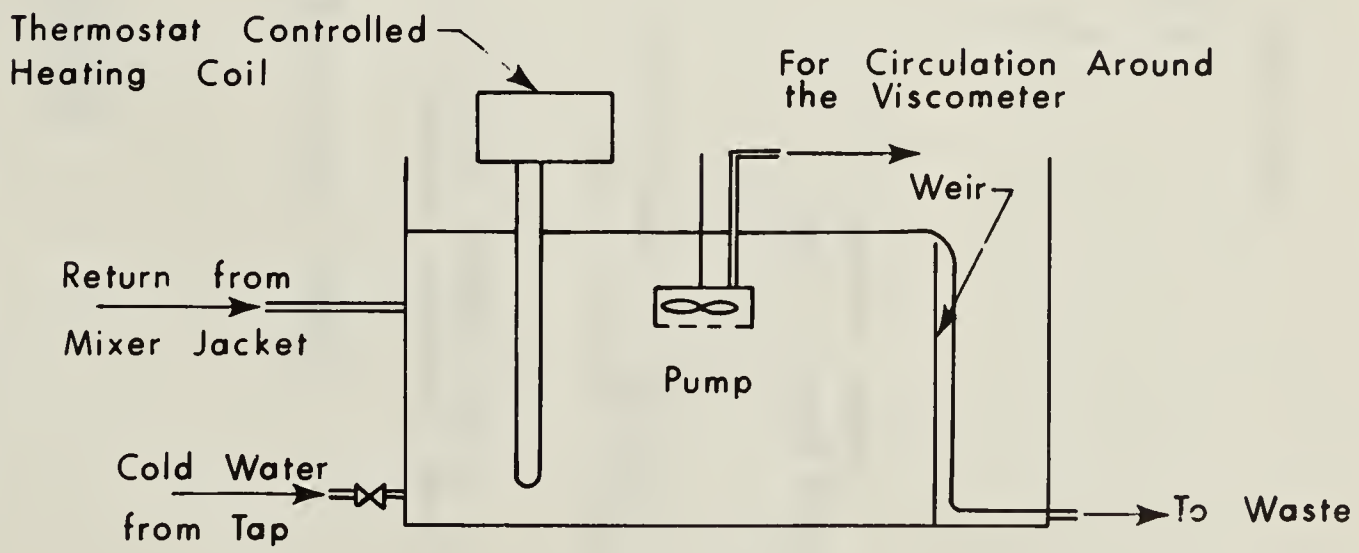

Fig. 8 Schematic Diagram of Constant Temperature Recirculation System

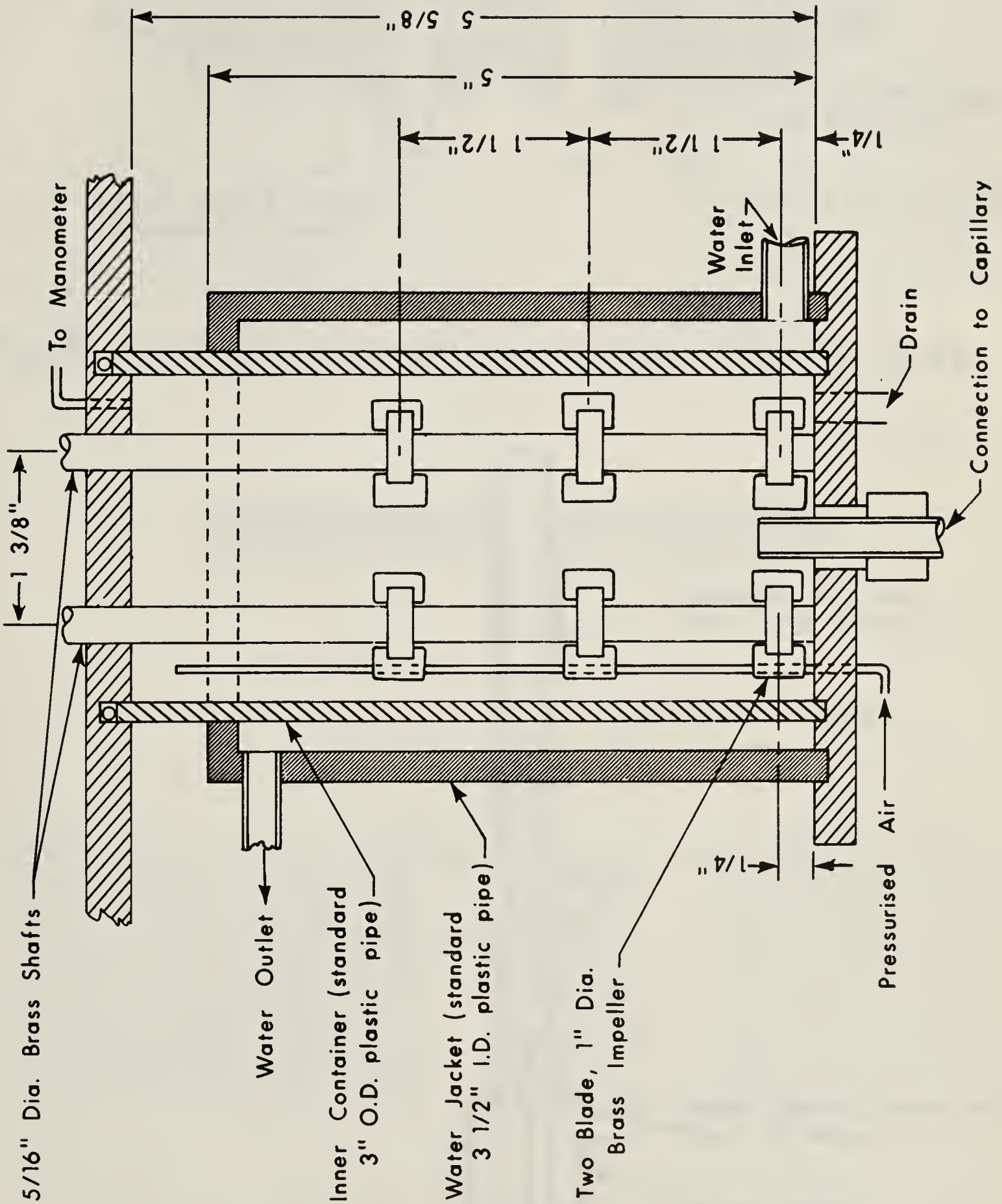

Fig. 9 Schematic Diagram of Mixer

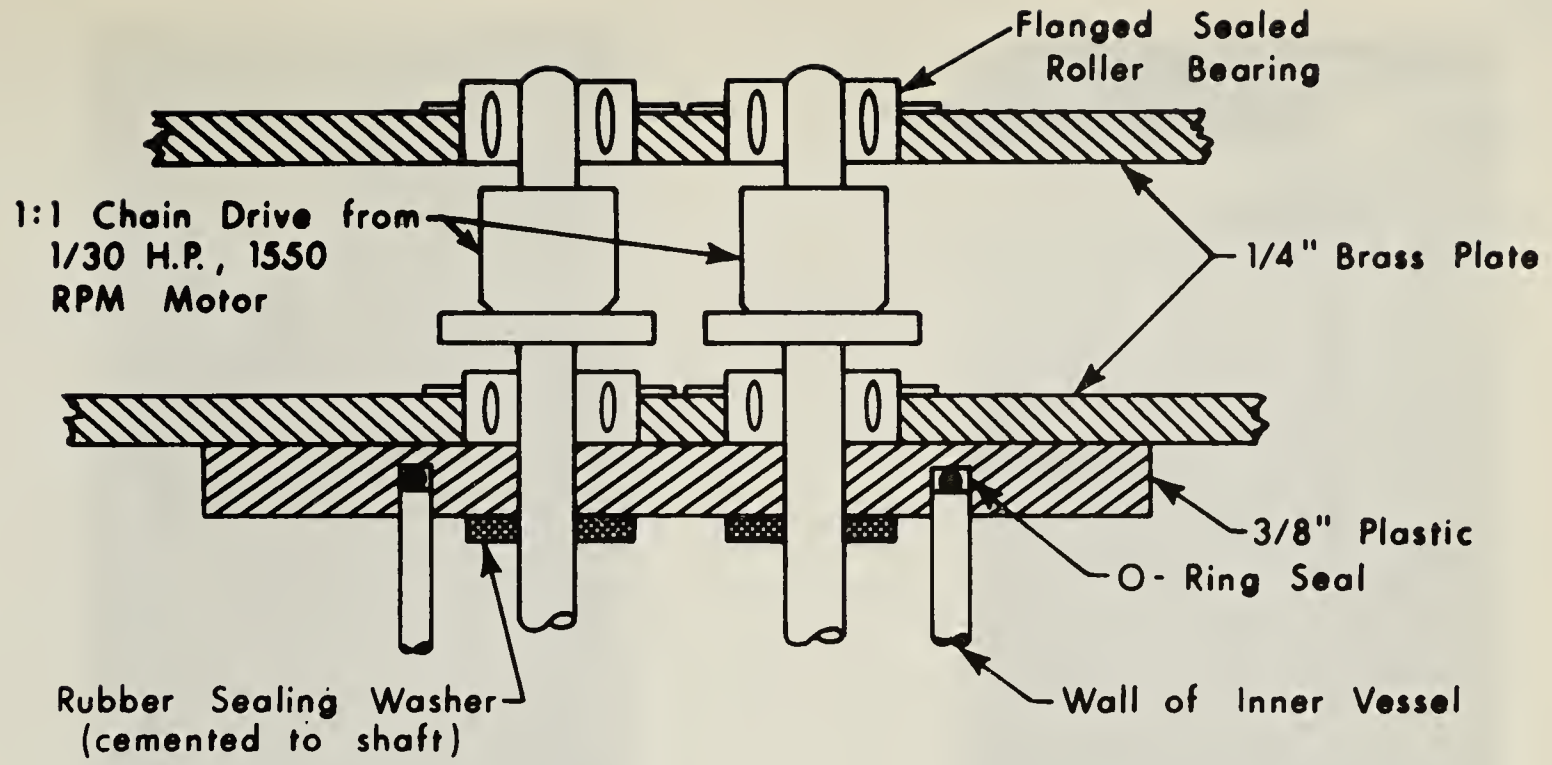

Fig. 10 Schematic Diagram of Bearings, Seal & Drive

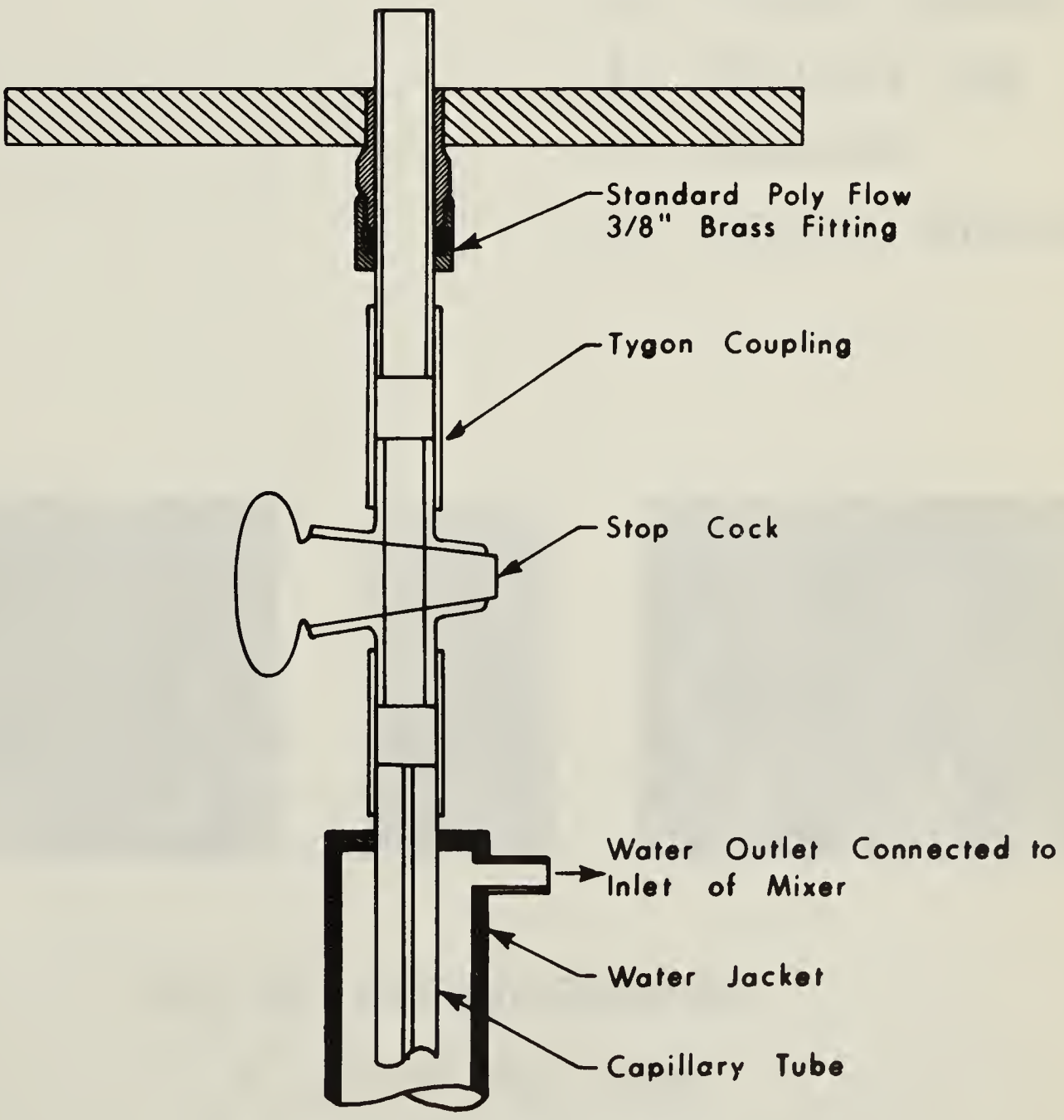

Fig. 11 Details of Capillary Tube Connection

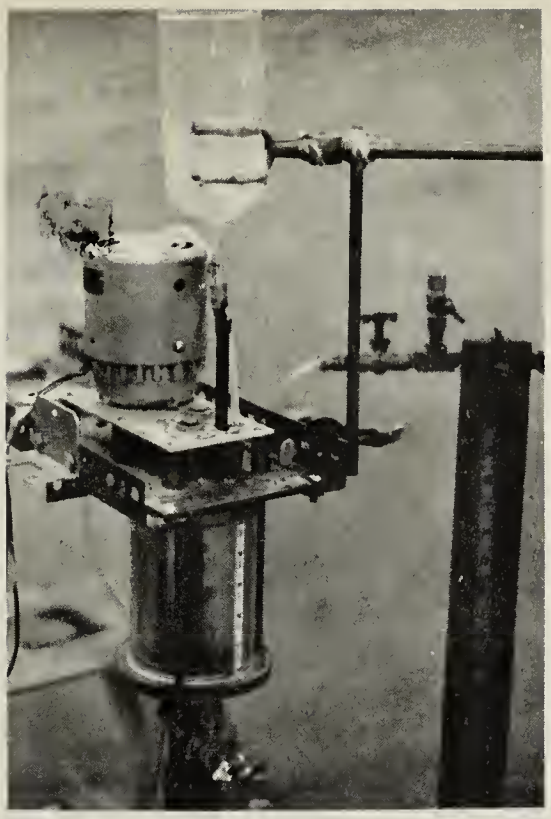

Fig. 13 THE STORAGE CHAMBER

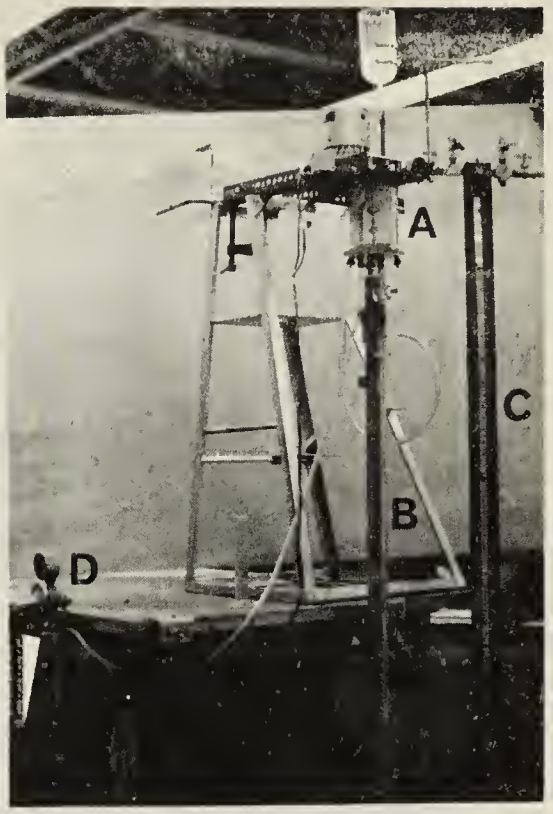

Fig. 12 THE EXPERIMENTAL SETUP

(A) STORAGE CHAMBER

(B) CAPILLARY TUBE

(C) MANOMETER

(D) PRESSURE REGULATOR

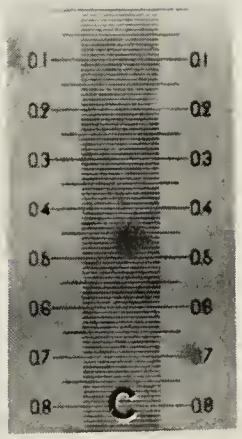

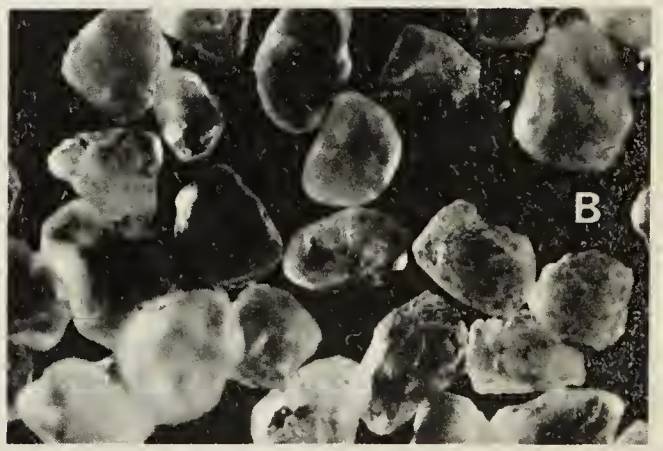

Fig. 16 PHOTOMICROGAPHS

A 60 - 70 MESH SAND

B 70 - 80 MESH SAND

C SCALE IN MM.

were used in the present investigation:

Tube A: 122 cm. long 2.0 mm dia.

B: 118 cm. long 2.7 mm dia.

The tubes were of glass. Each tube had a stopcock fused at one end and the entire length of tube was encased in a plastic water jacket and was mounted on a frame. The capillary tube was connected to the bottom of the storage chamber as shown in Fig. 11. The tube was set in perfect vertical position. The connection to the chamber and the tube was such that the tubes could be changed easily without disturbing the general setup.

3.2.4 DISCHARGE MEASUREMENT.

The discharge of the suspension through the capillary at the lower end of the tube was at atmospheric pressure. The flow was allowed to establish and then about 50 c.c. of the discharge was collected in a known interval of time in a container. The time was measured with an electrical stop-watch of accuracy 1/10 sec.

3.2.5 TEMPERATURE CONTROL

A constant temperature recirculating system, as in Fig. 9, was used to maintain the temperature of the liquid in the chamber at desired level. A thermostat controlled heating coil maintained the constant temperature in the water tank and a small pump circulated this water through the capillary tube jacket and the mixing chamber jacket. This arrangement gave a control of the temperature of the liquid in the

chamber to an accuracy of $\pm$ 1°F.

3.2.6 OPERATION.

The operation of the capillary viscometer is relatively simple. Once temperature is well under control the only readings to be taken are manometer reading, the average static head, and the volume of liquid issued in a known period of time. If the capillary length and the diameter are accurately known the elements of the flow curve $\tau_\omega = \frac{\Delta p\, D}{4 L}$ and $\frac{8V}{D}$ can be calculated.

However, it is very difficult to measure the diameter of a capillary accurately. Also, in the dilatant non-Newtonian fluid the pressure difference in a capillary tube is very sensitive to the diameter. Thus there is always a possibility of an error in the flow curve due to an error in the measurement of the diameter.

Also, the measured pressure difference will have to be corrected for (a) loss at entrance (b) loss at the valve and (c) the kinetic energy at the exit. But the magnitudes of these losses, especially in a non-Newtonian fluid flow, are difficult to predetermine and correct.

To overcome these difficulties an accepted method is to calibrate the instrument with stable Newtonian liquids of known viscosity. The calibration will be more meaningful if the ranges of shear rate and shear stresses used

in the calibration are comparable with those used in the investigation. The calibration, as discussed below, achieved this purpose quite satisfactorily.

3.2.7 CALIBRATION.

Two oils, M and N, whose exact viscosities at various defined temperatures were known accurately, were used to calibrate the two capillary tubes A and B. The viscosities of the oils were as follows:

TABLE: 2

VISCOSITIES OF THE CALIBRATING OILS

VISCOSITY IN C.P. AT	70°F	90°F	100°F
Oil M	4.532	3.372	2.939
Oil N	9.162	6.274	5.304

The flow rates at various pressures were measured (Tables A-1 to A-4) and the flow curve plotted as in Fig. 14, and Fig. 15. In these figures $\tau_{wm} = \frac{\Delta p\, D}{4L}$

where τ_{wm} = wall shear stress computed from

Δp = observed pressure difference

L = measured length of the capillary

D = measured diameter of the capillary

From the plots in Fig. 14 and 15, it is found that the observed viscosity is greater than the actual viscosity.

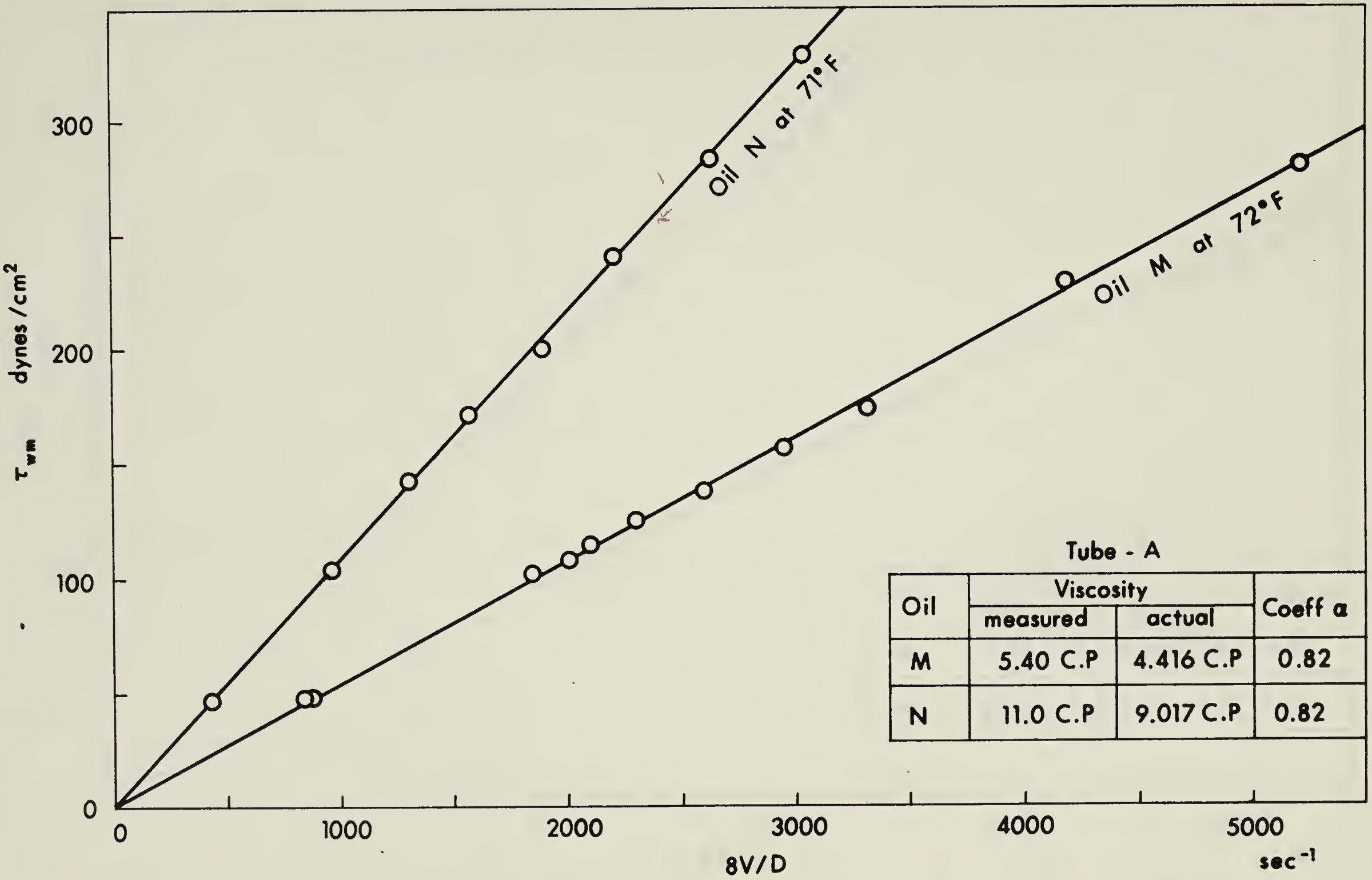

Tube - A

Oil	Viscosity		Coeff α
	measured	actual	
M	5.40 C.P	4.416 C.P	0.82
N	11.0 C.P	9.017 C.P	0.82

Fig. 14 Calibration of 2 mm Tube

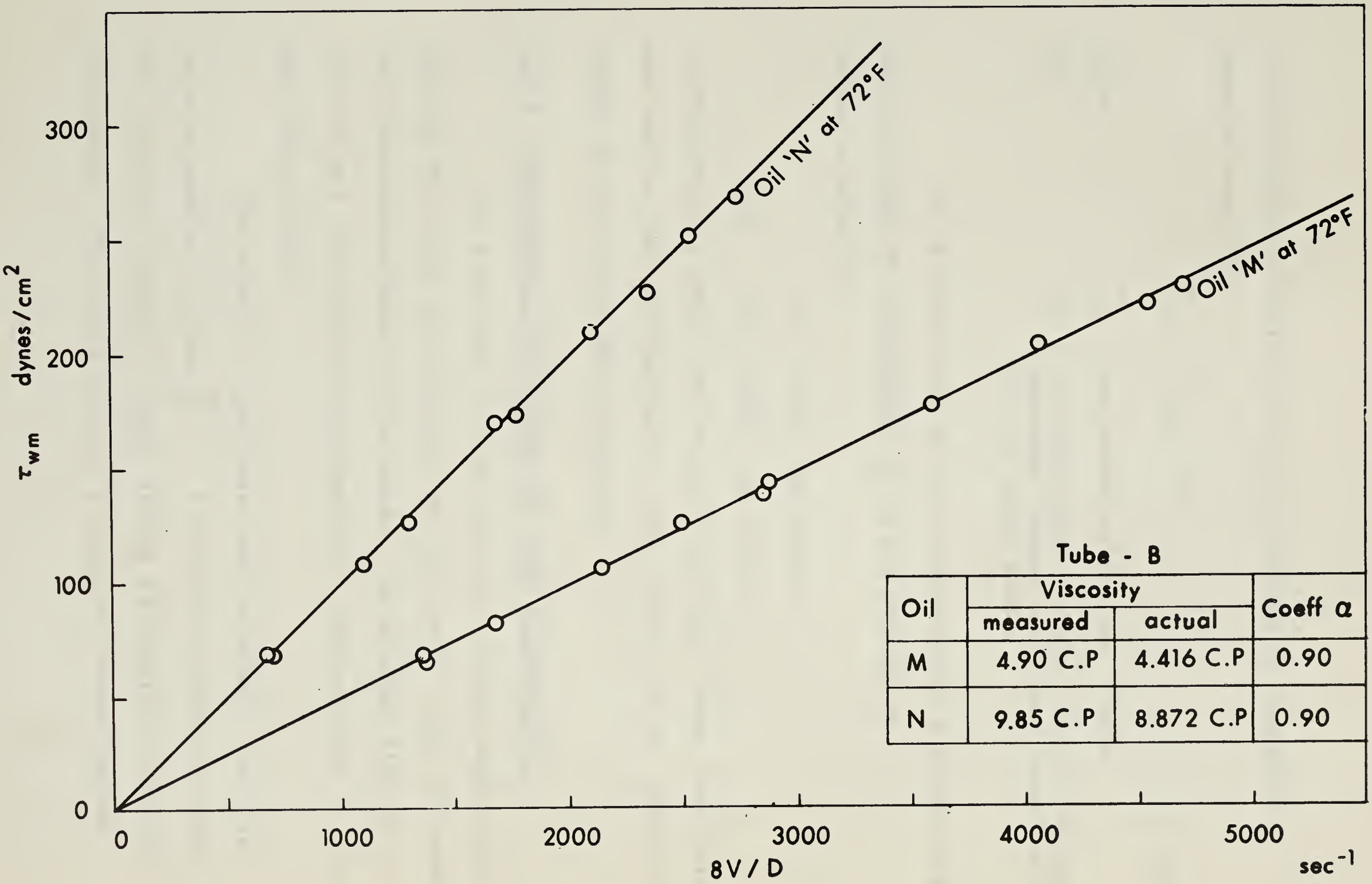

Tube - B

Oil	Viscosity		Coeff α
	measured	actual	
M	4.90 C.P	4.416 C.P	0.90
N	9.85 C.P	8.872 C.P	0.90

Fig. 15 Calibration of 2.7 mm Tube

By considering a correction to be applied to observed shear stress only

$$\tau_\omega = \tau_{\omega m} \cdot \alpha \qquad \text{- - - - - - (41)}$$

where τ_ω = corrected wall shear stress

and α = a coefficient to take care of various pressure losses and other inaccuracies in the measurement.

It is found that α is a constant for a given tube for the range of viscosities of oil M and oil N.

Hence, a value of

$\alpha = 0.82$ for tube A

and $\alpha = 0.90$ for tube B

is adopted as a result of the calibration. These coefficients are used in the calculation of shear stress of the suspensions tested in the capillary viscometer.

3.2.8 EXPERIMENTAL PROCEDURE FOR SAND SUSPENSIONS.

The sand used in the tests was Ottawa sand, passing through #60 sieve and retained on #80 sieve. Fig. 16 shows the photo-micrographs of the sand. The average size of d= 0.22 mm was accepted as representative and was used in all the calculations.

The object of the tests was to obtain the flow curve elements (τ_ω and $\frac{8V}{D}$) for various concentrations, over as wide a range of shear stress as possible with the instrument. The tests covered a range of concentration

from C = 0.13 to C = 0.35. All tests were performed at a constant temperature of 70°F.

In a typical test, corresponding to a concentration C_1, the quantity of dry sand and water required to make 450 c.c. of suspension of concentration C_1 was determined gravimetrically. The specific gravity of sand was assumed as 2.64. The required quantity of dry sand was placed in the filler and flushed in to the chamber with the previously calculated quantity of water. The mixture was brought to a suspension by turning on the agitator. The temperature was checked by drawing out a small quantity of the suspension by the drain valve. When the required constant temperature of 70°F was established, the chamber was pressurized to give the required shear stress. The capillary valve was then opened and some suspension allowed to drain-out to establish the flow. Then about 50 c.c. of the suspension was collected. The exact volume of suspension collected and the time taken were noted. Also the weight of the suspension was noted and the suspension dried in an oven and the weight of dry sand left was noted. From these measurements the exact concentration and the volume rate of flow were calculated. It was found that in the instrument the concentration intended and the exact concentration obtained in a test differed within $\pm$ 0.02. This was not considered as a serious defect as the object was to obtain the flow curve data over a range of concentrations.

Tables A-5 and A-6 give a summary of the data.

From the observed values of pressure drop the wall shear stress τ_ω is calculated as $\tau_\omega = \propto \tau_{\omega m}$. The flow function $\frac{8V}{D}$ is calculated from the discharge measurement. Tables A-7 and A-8 list the values of τ_ω and $\frac{8V}{D}$ and other calculated quantities corresponding to various experiments.

CHAPTER IV

INTERPRETATION OF DATA

4.1 SHEAR STRESS - FLOW FUNCTION RELATIONSHIP

Flow curves, i.e., Plots of wall shear stress against flow function defined by $\frac{8V}{D}$, are the basis for studying rheological behaviour from capillary viscometer data. Fig. 17 shows a plot of shear stress τ_ω and the flow function $\frac{8V}{D}$, on an arithmetic scale. The concentration C is used as the third parameter. All the data obtained from both the tubes A and B are plotted. By interpolation among plotted points, lines representing the relationship between τ_ω and $\frac{8V}{D}$, and having a constant value of C, are drawn. Five such lines having a value of C = 0.13, 0.19, 0.26, 0.29 and 0.34 are shown in Fig. 17. It can be seen that these lines are curves with concave curvature towards the τ_ω axis and thus indicate the non-Newtonian behaviour of the suspension.

As a first approximation, it was assumed that at very low shear rates the fluid behaviour can be approximated to that of a Newtonian fluid. With this assumption the relative viscosities of the suspension, corresponding to various concentration lines, were calculated at the lowest shear rate up to which the lines can be reasonably extrapolated. These values were then compared with the formulas of Vand (equation 32) and Mooney (equation 31) which have been recommended by Rutgers (16) as applicable

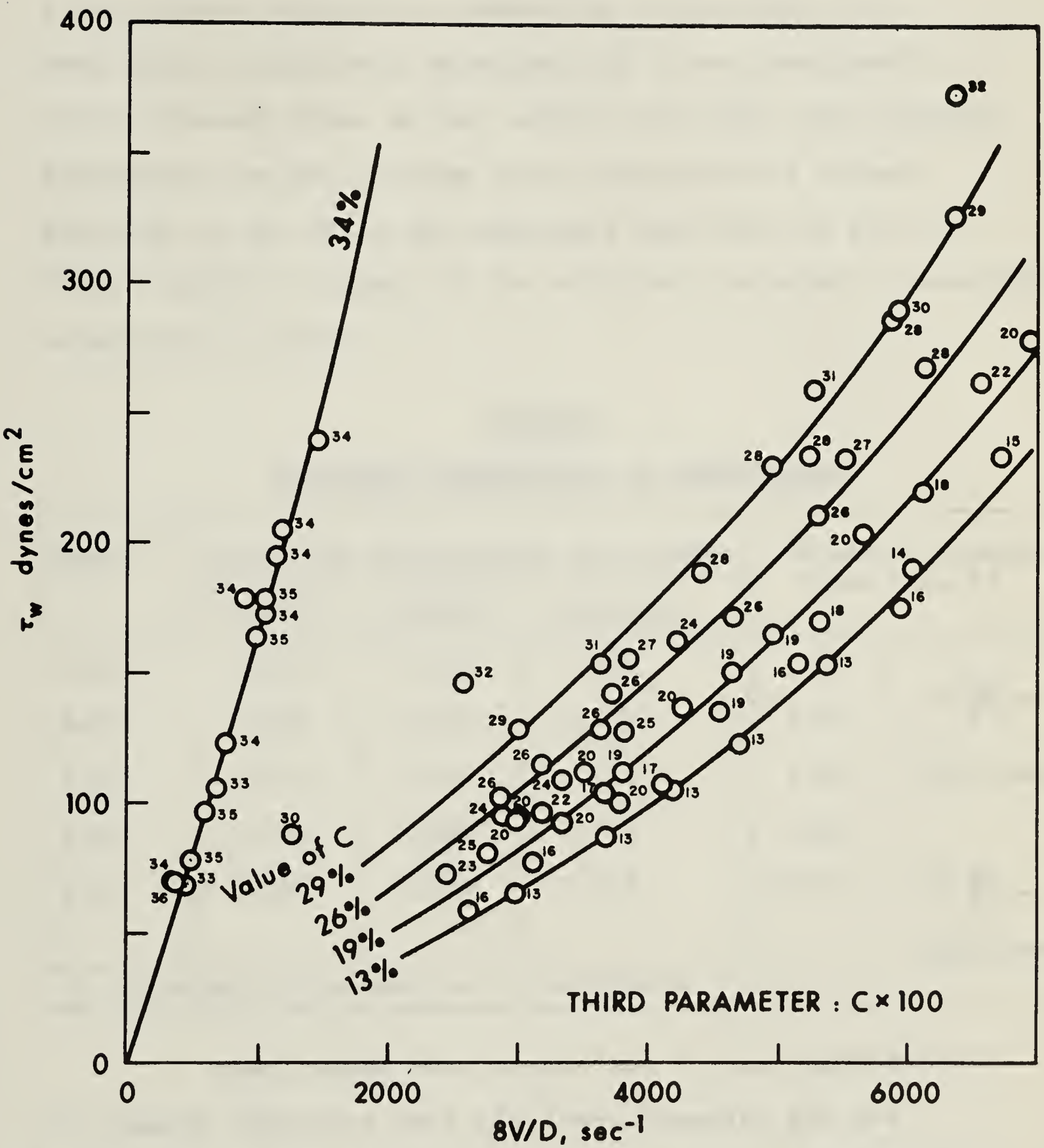

Fig. 17 Plot of τ_w vs 8V/D (Arithmetic Scale)

to the entire concentration range of the suspension of rigid spheres behaving as Newtonian fluid (sec. 2.1). Even though Einstein's (equation 29) is not applicable to the present case, it was used to calculate the relative viscosities to get an idea of the variation of values obtained by the other two equations and from the Fig. 17. Table 3 gives a summary of the relative (to water) viscosities calculated as above.

TABLE:3

RELATIVE VISCOSITIES OF SUSPENSIONS

Concn. C	Relative Viscosities by Formula			Relative Viscosity from fig. 17	
	VAND	MOONEY	EINSTEIN		
0.13	1.328	1.480	1.325	1.85	At $\frac{8V}{D}$ = 2000 Sec.$^{-1}$
0.19	1.480	1.920	1.475	2.50	
0.26	1.645	2.770	1.650	3.30	
0.29	1.780	3.380	1.750	4.25	
0.34	2.080	5.580	1.850	16.70	At $\frac{8V}{D}$ = 1000 Sec.$^{-1}$
η of water is assumed as 1 centipoise					

Even though this comparison is very approximate it clearly indicates that the above formulas are not applicable to the conditions of the present investigation. The pronounced effect of concentration on the characteristics of the suspension is apparent from the Fig. 17.

Since the behaviour of the suspension is non-Newtonian, a better method of representing the Capillary Viscometer data is to plot τ_ω vs $\frac{8V}{D}$ in a logarithmic plot. It can then be analyzed in the light of the non-Newtonian fluid behaviour discussed in sec. 1.3.

4.2.1 ANOMALOUS FLOW

From the nature of the data collected in the present investigation, it was not possible to apply Oldroyd's method (sec. 1.4.1) to determine effective slip velocity at the wall. It is assumed that there is no anomalous behaviour of the suspension.

4.2.2 PARTICLE SLIP VELOCITY

The particle slip velocity (sec. 1.4.2) can approximated to the free fall velocity at low concentration of solids. The free fall velocity W_f of the sand size d = 0.22 mm is 2.80 cm/sec. In the concentration range C = 0.13 to 0.30 the velocities of the suspension in the tests were between 60 cm/sec. to 210 cm/sec. Thus, if it is assumed that the particle slip velocity in this concentration range is 2.80 cm/sec., it will be a small fraction of the velocity of the suspension. Hence, it is assumed to be too small to affect concentration measurements.

However, in the concentration range C = 0.30 to 0.35 the velocities of the suspension were between 10 cm/sec. and 40 cm/sec. From Fig. 17 it can be seen that there is a

pronounced effect of concentration of solids which has increased the relative viscosity of the suspension to as high a value as 16. It is therefore felt proper to assume the particle slip velocity, at this high concentration range, to be given by the hindered settling velocity. The following empirical formula has been recommended by Badger and Banchero (24) for the calculation of hindered settling velocity of spherical particles of uniform size;

$$W_h = W_f \psi(\epsilon) \qquad \text{------ (42)}$$

where W_h = hindered settling velocity

W_f = free settling velocity

ϵ = volume concentration of voids = 1 - C

$\psi(\epsilon) = \epsilon^{2 \times 10^{-1.82(1-\epsilon)}}$ for values of ϵ between 0.95 and 0.50.

Assuming this formula to be applicable to the sand used in the tests, the hindered settling velocity of the sand at C = 0.33 is calculated as;

For C = 0.33

ϵ = 0.67

$\psi(\epsilon) = (0.67)^{2 \times 10^{-1.82(0.33)}} = 0.113$

W_f = 2.80

W_h = 2.80 x 0.113 = 0.316 cm/sec.

Considering this as the representative particle slip velocity in the concentration range C = 0.30 to 0.35, it will be noticed that the particle slip velocity is

between 3% to 0.75% of the velocity of the suspension in this range. Hence it is assumed too small to affect the measured concentration values.

4.3 LOGARITHMIC FLOW CURVE

Fig. 18 is a logarithmic plot of τ_ω against $\frac{8V}{D}$. All the data shown in Fig. 17 are plotted but the concentration values have been stated at intervals of 0.03 and then marked distinctively. It can be seen that for a given value of concentration the variation of τ_ω with $\frac{8V}{D}$ can be represented by a straight line. Even though there is a slight scatter of data the trend is very clear.

For concentrations up to 0.30 the lines of constant C are parallel. Thus they can be expressed as

$$\tau_\omega = K' \left(\frac{8V}{D} \right)^{n'} \qquad \text{- - - - - - (22)}$$

The value of K' depends upon the value of C. It is found that n' = 4/3, indicating that the behaviour of the suspension is dilatant in the range of shear rates tested.

In the concentration range C = 0.30 to 0.35, there is a sudden change in the characteristics of the fluid. The line C = 0.35 is still straight but the value of n' is 1.04. The value of K' has undergone a sudden increase.

The lowest concentration tested was 0.13. The non-Newtonian behaviour is evident at this concentration also for shear stress values greater than 50 dynes/cm^2

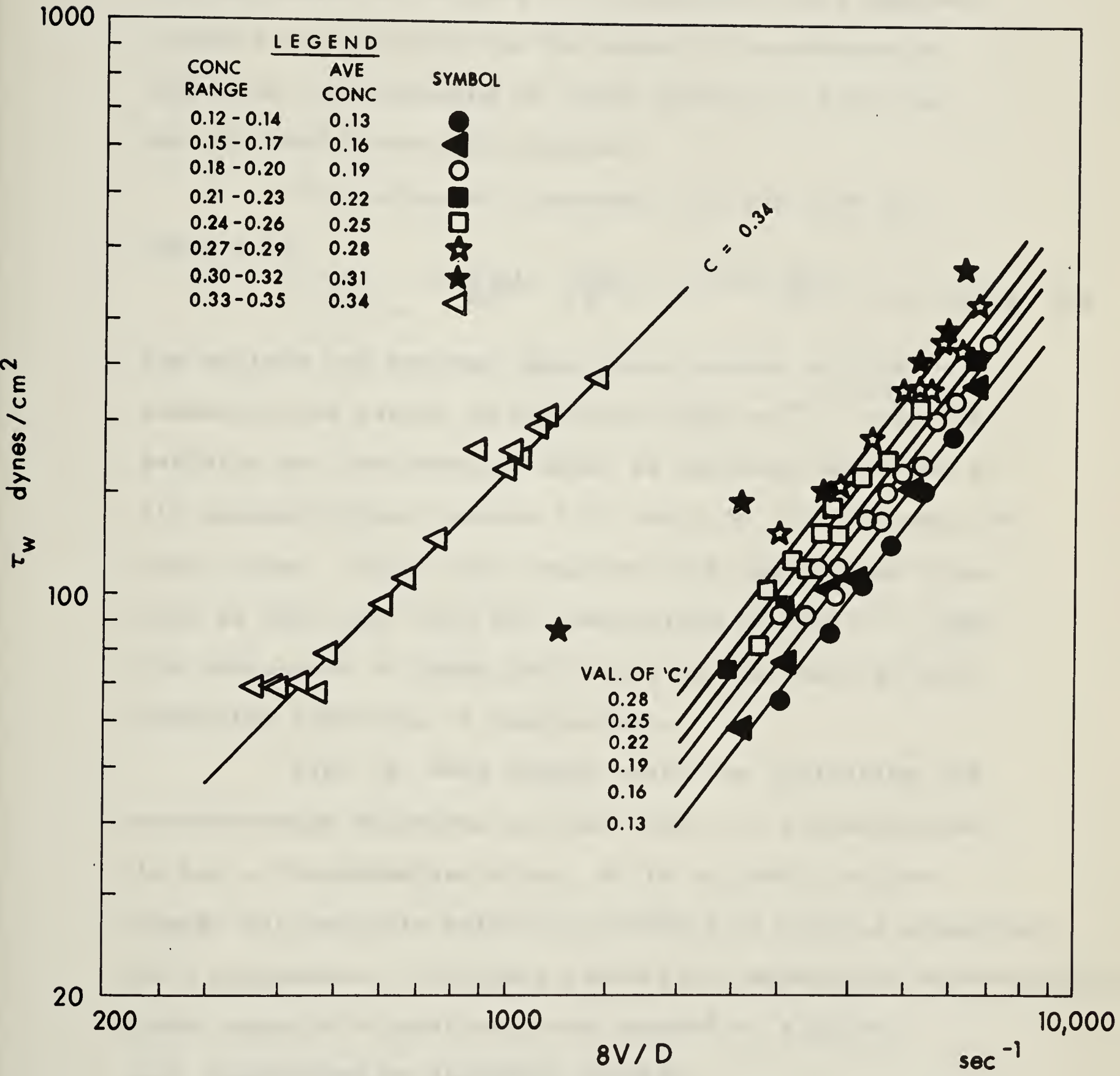

Fig. 18 Plot of τ_w vs. 8V/D (Logarithmic Scale)

and flow function value greater than 2500 sec^{-1}. Thus the conclusion of Rutgers (17) that 25% volume concentration as the minimum for the onset of non-Newtonian behaviour of suspension of rigid spheres is not true for the sand suspensions tested.

For values of C between 0.13 and 0.30 the shear rate

$$\left(-\frac{\partial u}{\partial r}\right)_w = \frac{3n'+1}{4n'}\left(\frac{8V}{D}\right) = 0.94\left(\frac{8V}{D}\right) \quad \text{- - -(Equn. 21)}$$

The minimum and maximum shear rates tested in this concentration region are therefore 2300 sec^{-1} and 6500 sec^{-1}. There is definite and unmistakable proof of dilatant behaviour at all concentrations between 0.13 and 0.30 in this range of shear rates. This, when compared with the maximum shear rate of 1300 sec^{-1} and the conclusions of Table: 1, show the importance of shear rate value on the onset of non-Newtonian behaviour of suspensions.

Fig. 18, even though useful in indicating the non-Newtonian behaviour and the effect of concentration, is not a dimensionless plot. So is unlikely to give simply the possible relative influence of various parameters of a suspension. To obtain potentially meaningful dimensionless terms Bagnold's hypothesis was adopted as a guide.

4.4 ADAPTATION OF BAGNOLD'S CONCEPT

The essence of Bagnold's concept (Sec. 2.3) is the recognition of the shear and direct stresses due to impact of grains and its unique correlation with $\frac{du}{dy}$, λ,

ρ_s and d. However, his experiments were conducted with uniform shear strain throughout the flow, i.e., $\frac{du}{dy}$ = constant, and with specific gravity of the spheres same as that of the fluid. In the present investigation the velocity gradient is not constant across the tube, the particles are not spherical and $\rho_s = 2.64$ gm/cm^3 and $\rho_f = 1.00$ gm/cm^3.

In the following analysis the concentration range C = 0.13 to 0.30 is considered as the range of interest. The same analysis is however applied to the range C = 0.30 to 0.35 even though the behaviour in this range may be different.

In Fig. 18, it has been shown that τ_ω and $\frac{8V}{D}$ follow the equation

$$\tau_\omega = K' \left(\frac{8V}{D}\right)^{n'} \qquad \text{- - - - - - (22)}$$

and that n' is constant at 4/3 for various concentrations up to 0.30. Hence, in the range of shear rates tested the 'power law' and equation 16 are applicable.

$$n' = n = 4/3$$

$$K' = K\left(\frac{3n+1}{4n}\right)^n \qquad \text{- - - - - - (22a)}$$

$$K = fn\ (C)$$

From equation 17, $\left(-\frac{\partial u}{\partial r}\right) = \frac{3n+1}{4n}\left(\frac{8V}{D}\right)\left(\frac{r}{R}\right)^{1/n}$

and hence the average shear rate is proportional to $\frac{8V}{D}$.

Also the maximum shear rate is given by

$$\left(-\frac{\partial u}{\partial r}\right)_{max} = \left(-\frac{\partial u}{\partial r}\right)_w = \frac{3n+1}{4n}\left(\frac{8V}{D}\right)$$

$$\text{i.e. } \left(-\frac{\partial u}{\partial r}\right)_\omega \propto \frac{8V}{D}$$

Thus the average shear rate and the maximum shear rate are proportional to $\frac{8V}{D}$. It follows therefore that the term $\frac{8V}{D}$ adequately represents the shear rate in the tube.

Suppose the total shear stress in the capillary is considered to be made up of two parts

$$\tau_w = \tau_f + \tau_s \qquad \text{------ (44)}$$

Where τ_s = Shear stress due to the presence of solids in the suspension as per Bagnold's concept.

τ_f = Shear stress due to the flow of the liquid medium alone.

As a first approximation assume

$$\tau_f = \eta \left(\frac{8V}{D}\right) \qquad \text{------ (45)}$$

Where η = coefficient of dynamic viscosity of the Newtonian liquid

$$\tau_s = \tau_w - \eta \left(\frac{8V}{D}\right) \qquad \text{------ (45a)}$$

Now the grain shear stress should depend upon the characteristics of

(a) Solids in suspension: size d, shape, density ρ_s, concentration C.

(b) Liquid suspending medium: density ρ_f, viscosity η.

(c) Flow: the flow function $\frac{8V}{D}$.

$$\tau_s = Fn \left(d, \rho_s, C, \text{Shape factor}, \rho_f, \eta, \frac{8V}{D}\right) \qquad \text{------ (46)}$$

The linear concentration λ is considered as a better representative parameter of the crowding effect of the particles than the volume concentration C. Replacing C by λ, as has

been done by Bagnold,

$$\tau_s = \text{Fn}\left(d, \rho_s, \lambda, \rho_f, \eta, \frac{8V}{D}, \text{Shape factor}\right) \quad \text{- - - - - - (47)}$$

By dimensional analysis,

$$\frac{\tau_s \rho_s d^2}{\eta^2} = \text{fn}\left[\lambda, \frac{(\frac{8V}{D})\rho_s d^2}{\eta}, \frac{\rho_f}{\rho_s}, \text{Shape factor}\right] \quad \text{- - - - - - (48)}$$

These dimensionless groups must be functionally related, if the hypothesis is correct. In the present investigation ρ_f/ρ_s and shape factor were constant for all experiments. So, $\frac{\tau_s \rho_s d^2}{\eta^2}$ is plotted against $(\frac{8V}{D})\frac{\rho_s d^2}{\eta}$ with λ as a third parameter, in Fig. 19. It can be seen that for a given value of λ, there is a good correlation of the two parameters. The relationship is linear for most part of the plot i.e. for values of $(\frac{8V}{D})\frac{\rho_s d^2}{\eta}$ up to 600.

Thus for a constant value of λ in this region

$$\frac{\tau_s \rho d^2}{\eta^2} = K_1 \left(\frac{8V}{D}\frac{\rho_s d^2}{\eta}\right)^m \quad \text{- - - - - - (49)}$$

The value of m = 5/3 for $\lambda < 3.5$

and m = 1.04 for $\lambda > 4.0$

Also $K_1 = \text{fn}(\lambda)$

Table: 4 shows the value of K_1 calculated from Fig. 19 for various value of λ. To find the functional relation between K_1 and λ, K_1 is plotted against λ in Fig. 20. For values of $\lambda < 3.5$, there is a clear indication that

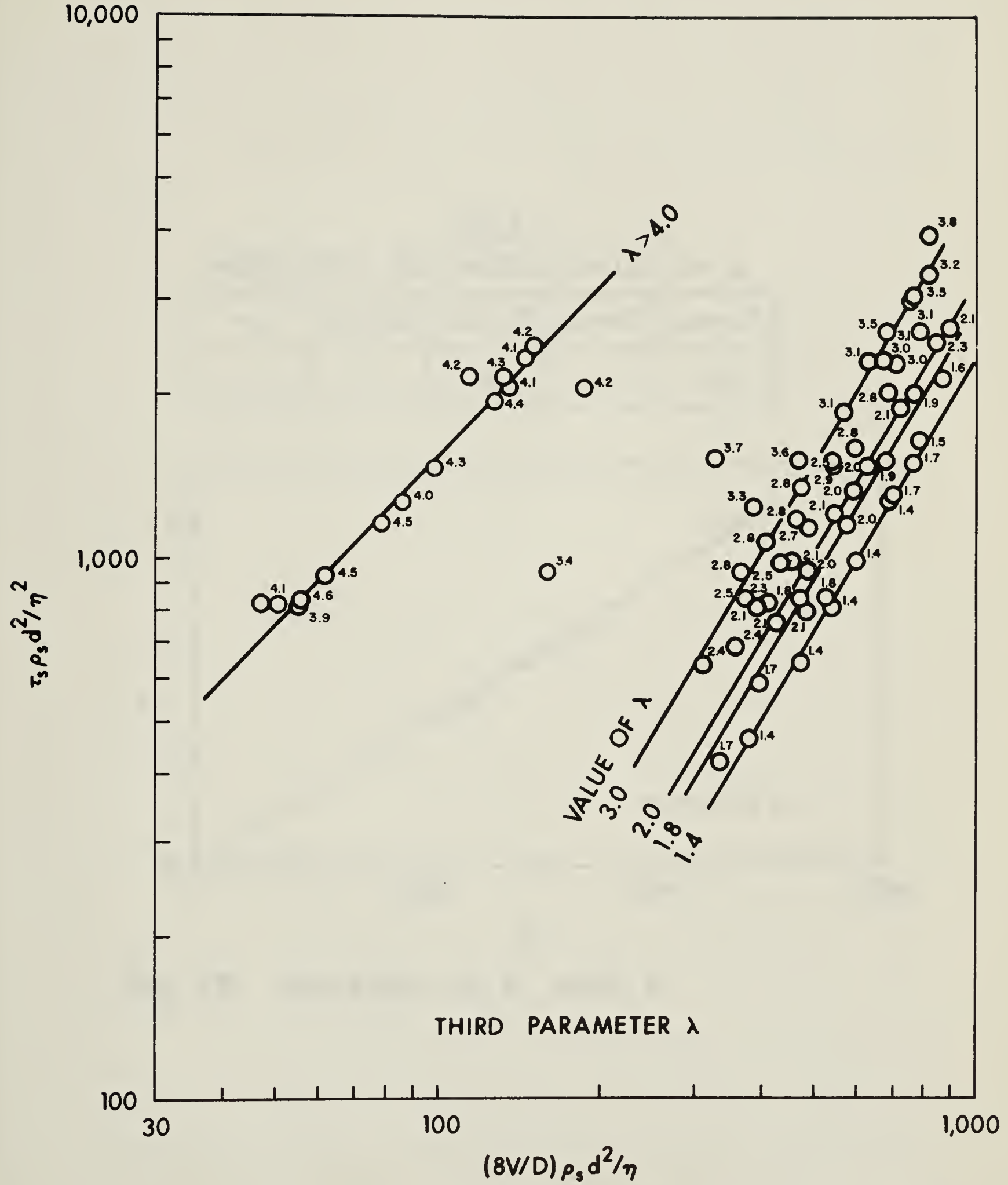

Fig. 19 Variation of $\tau_s \rho_s d^2/\eta^2$ with $(8V/D)\rho_s d^2/\eta$ and λ

TABLE 4

VALUES OF K_1 FOR VARIOUS VALUES OF λ

K_1	2.35×10^{-2}	2.85×10^{-2}	3.25×10^{-2}	4.65×10^{-2}
λ	1.4	1.8	2.0	3.0

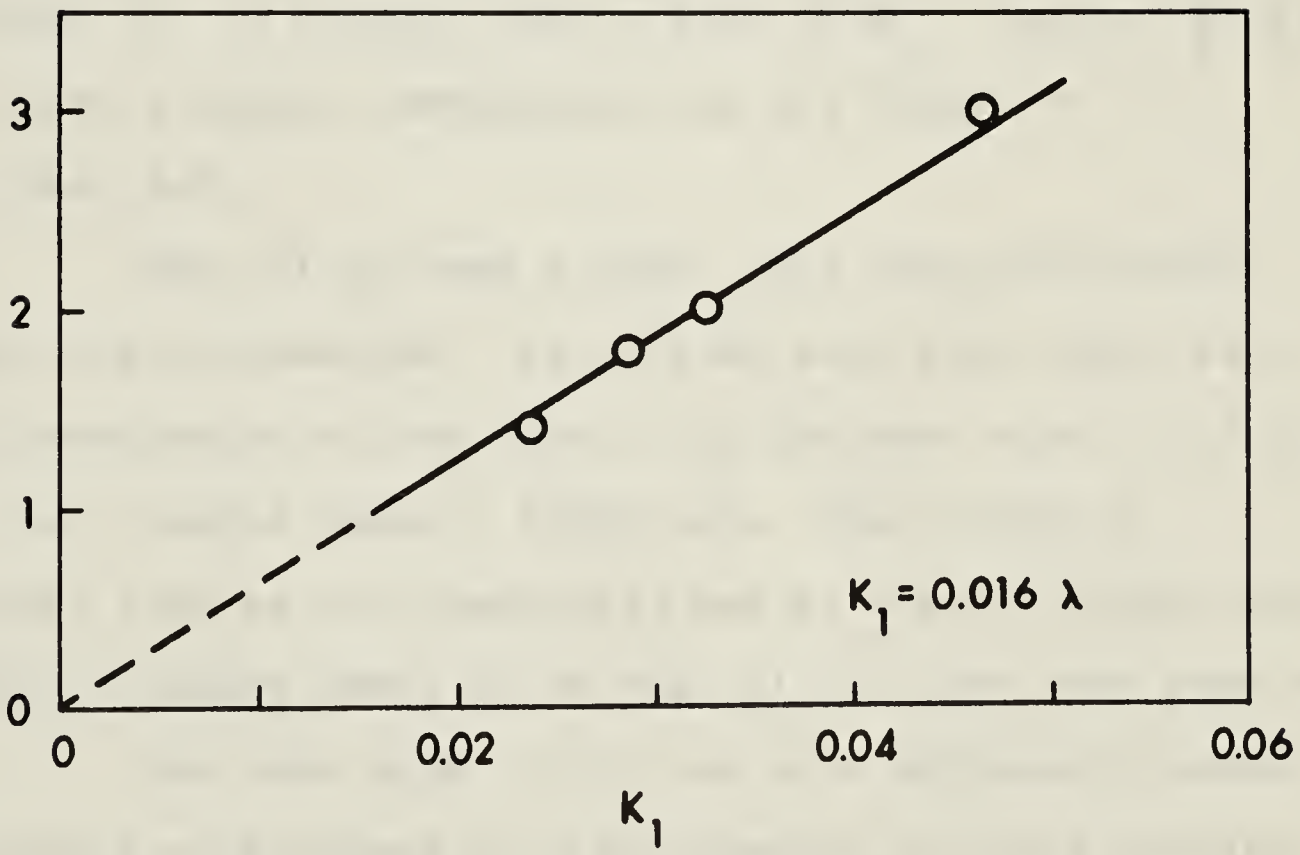

Fig. 20 Variation of K_1 with λ

$$K_1 = K_2 \cdot \lambda \qquad \text{- - - - - - (50)}$$

Where K_2 is a constant. From fig. 20 $K_2 = 0.016$.

Thus for $\lambda < 3.5$, and $\frac{\rho_f}{\rho_s}$ and shape factor being constant

$$\frac{\tau_s \rho_s d^2}{\lambda \eta^2} = K_2 \left[\frac{8V}{D} \frac{\rho_s d^2}{\eta} \right]^m \qquad \text{- - - - - - (51)}$$

It is interesting to note that $\frac{\tau_s \rho_s d^2}{\lambda \eta^2}$ is the same as the parameter G_T^2 used by Bagnold. From equation 51 it follows that a plot of G_T^2 against $\frac{8V}{D} \frac{\rho_s d^2}{\eta}$ must give a unique correlation for all values of λ less than 3.5.

Fig. 21 is such a plot. All the experimental points are represented. It will be seen that there is a good correlation of the data. All the data with $\lambda < 3.5$ fall on a single curve - (Curve A). Even though a straight line as per equation 51 can be drawn through these points, a smooth curve as in Fig. 21 fits the data very well.

The data with $\lambda > 3.5$ are in a different regime. The points with values of $\lambda > 4.0$ seem to follow a relation similar to those with $\lambda < 3.5$.

It is interesting to observe that the values of G_T^2 of all the data fall between 180 to 1500. This corresponds to the transition region between viscous and inertial zones of grain shear indicated in Fig. 6.

Consider the curve A ($\lambda < 3.5$). Even though the

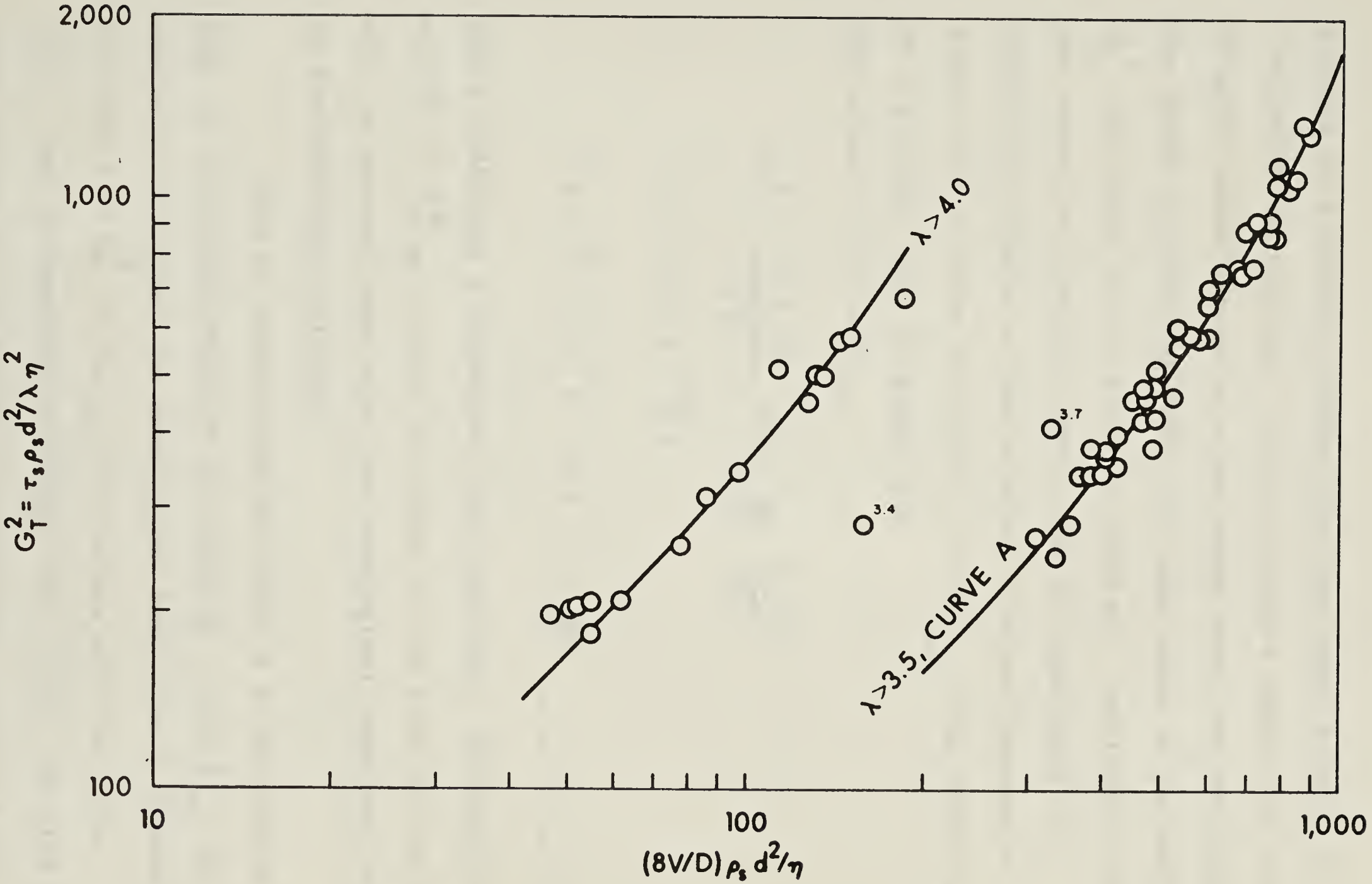

Fig. 21 Plot of G_T^2 Against $(8V/D)\rho_s d^2/\eta$

abscissa is different between this and curve in Fig. 6, the similarity is striking. Both the curves depict the variation of grain shear stress with the shear rate, but the nature of the shear is different. For the same range of the ordinate G_T^2 the shape of the curve is similar. Considering both the curves as similar, curve A can be considered as a transition between a line of slope 1.00 and another of slope 2.00 as shown in Fig. 22. At $G_{T\ cr}^2$ the curve changes to a straight line of slope 1.0.

For values of $G_T^2 \leq G_{T\ cr}^2$

$$G_T^2 = \frac{\tau_s \rho_s d^2}{\lambda \eta^2} = K_* \left[\frac{8V}{D} \quad \frac{\rho_s d^2}{\eta} \right]$$

$$\tau_s = K_* \lambda \eta \left(\frac{8V}{D} \right)$$

$$\tau_w = \tau_f + \tau_s = \left[1 + K_* \lambda \right] \eta \cdot \frac{8V}{D} \qquad \text{- - - - - - (52)}$$

which indicates a Newtonian flow behaviour. Similarly for all $G_T^2 > G_{T\ cr}^2$, since the slope of the line in Fig. 22 will be greater than unity the rheological behaviour would be non-Newtonian dilatant.

Thus by considering the curve A to be similar to Fig. 6, a critical value of the term G_T^2 i.e. $G_{T\ cr}^2$ can be envisaged such that the rheological behaviour is Newtonian for values of $G_T^2 \leq G_{T\ cr}^2$. For values of $\lambda < 3.5$ this $G_{T\ cr}^2$ may be expected to depend upon ρ_f/ρ_s and also the shape factor of the solids in suspension. For $\lambda > 3.5$ a

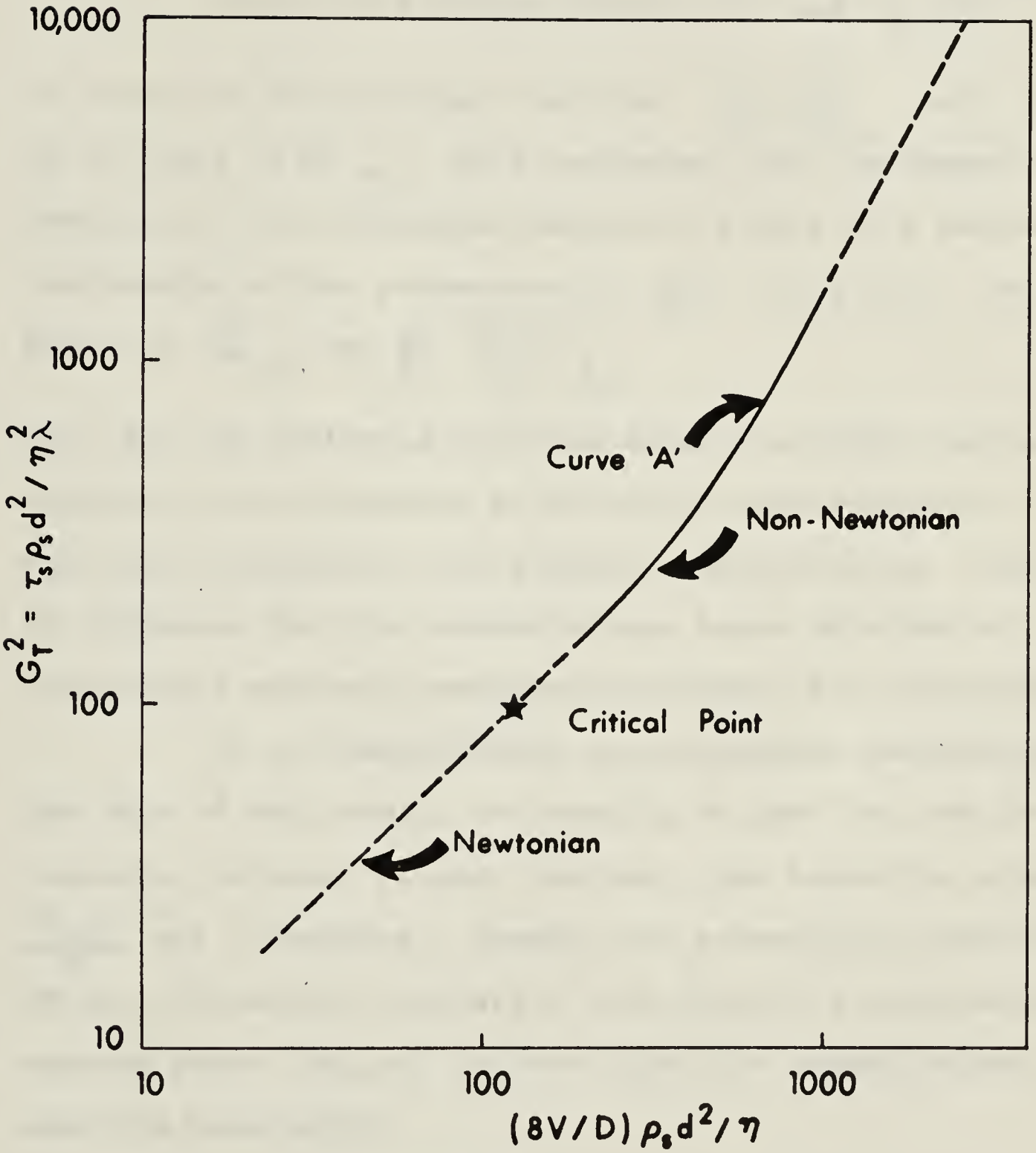

Fig. 2.2 Extrapolation of Curve 'A'

similar relation may exist, but the experimental data is scanty to warrant any conclusions.

Since the relation between G_T^2 and $\frac{8V}{D}\frac{\rho_s d^2}{\eta}$ is unique it follows that the term $\frac{8V}{D}\frac{\rho_s d^2}{\eta}$ will also be critical at $G_{T\ cr}^2$. This indicates that the change from Newtonian to non-Newtonian behaviour occurs at a unique combination of the parameters τ_w, $\frac{8V}{D}$, λ, ρ_s, d, η as given by $G_{T\ cr}^2$ or $\left(\frac{8V}{D}\frac{\rho_s d^2}{\eta}\right)_{cr}$

Thus Fig. 22 indicates that the Bagnold's theory can be applied to the behaviour of practical suspensions in capillary viscometer with suitable modifications. Also, it indicates that the dimensionless terms obtained by dimensional analysis adequately represent the phenomenon.

It is realised that in the present investigation the size of the sand d, the density of sand ρ_s, and the viscosity of water η, were constant, and hence the product $\frac{\rho_s d^2}{\eta}$ was a constant. However the encouraging correlation of Fig. 22 and its similarity with Bagnold's experimentally derived curve (Fig. 6) indicate that the dimensionless terms used are meaningful.

4.5 CRITICAL CONCENTRATION

Figs. 17, 18, indicate that while the behaviour of the suspension in the concentration range 0.13 to 0.30 follow a particular trend there is a sudden change in the characteristics between C = 0.30 and 0.35. Even though the

region C = 0.13 to 0.30 was the region of interest in the previous analysis the experimental points with C > 0.30 are all included in the analysis and the plots. It is clear from figs. 17 through 22 that there exists a separate regime of behaviour for C > 0.30 but the experimental data are insufficient to predict the behaviour in this region.

Also, the existence of a critical concentration between C = 0.30 and 0.35 is clear from the above plots. This phenomenon of critical concentration has been observed by several investigators. The various observations and the explanations advanced for this behaviour have been reviewed in sec. 2.4. The observed value of C_{cr} between 0.30 and 0.35 is within the range of values of 0.30 and 0.50 at which this phenomenon has been observed by various investigators.

CHAPTER V

CONCLUSIONS AND RECOMMENDATIONS

5.1 CONCLUSIONS

The capillary viscometer developed in the laboratory is well suited for the analysis of the rheological characteristics of suspensions. The tests on the sand-water suspension show that systematic testing can be carried out over a very wide range of shear rates in such equipment to get useful and sufficiently accurate data.

The review of the literature on flow characteristics of suspensions indicate that the available information is insufficient to predict the performance of a suspension in a practical case. Also in most of the theoretical and empirical works there is a lack of full appreciation of some of the factors influencing the behaviour of the suspension. The Bagnold's concept of grain shear stress is a new approach and seems to have considerable potential of application.

The tests on sand-water suspension indicate that in the range of shear rates 2300 - 6300 sec^{-1} the suspension is non-Newtonian dilatant at all concentrations greater than 0.13. Using Metzner's method of describing the capillary viscometer data, it is found that the suspension behaves as a powerlaw fluid with n = 4/3 for values of C between 0.13 to 0.30.

The results of the dimensional analysis when

applied to the test data indicate that the dimensionless number $G_T^2 = \frac{\tau_s \rho_s d^2}{\lambda \eta^2}$ has a unique functional relationship with the term $\left(\frac{8V}{D}\frac{\rho_s d^2}{\eta}\right)$ for a concentration range $\lambda < 3.5$. By considering the similarity of this functional relationship and that between G_T^2 and N as found by Bagnold, a critical number $G_{T\,cr}^2$ can be envisaged to mark the transition from Newtonian to non-Newtonian flow regime of the suspension.

A critical concentration at which an abrupt change in the characteristics of the suspension take place is noticed between C = 0.30 and 0.35.

5.2 RECOMMENDATIONS

It is recommended that:

(a) a systematic study be carried out by varying the parameters over a wider range to prove conclusively the validity and limitations of the above conclusions.

(b) a similar study be made for turbulent flow through vertical tubes.

LIST OF REFERENCES

1. Metzner, A.B. — "Non-Newtonian Technology" - A chapter in "Advances in Chemical Engineering" - Ed. by Drew, T.B. and Hoopes, J.W. Academic Press, Inc., N.Y. 1956.

2. Metzner, A.B. — "Flow of Non-Newtonian Fluids"- Sec. 7 in "Handbook of Fluid Dynamics"- Ed. by Streeter, V.L. McGraw-Hill Inc., N.Y. 1961.

3. Wilkinson, W.L. — "Non-Newtonian Fluids" Pergamon Press, 1960.

4. Reiner, Markus — "Deformation, Strain and Flow"- Interscience Publishers Inc., N.Y. 1960.

5. Govier, G.W. — "Interpretation of Rheological data"- The Journal of the Engineering Institute of Canada, March, 1960.

6. Behn, V.C. — "Derivation of Flow Equations for Sewage Sludges", Journal of Sanitary Engineering Division, Proc. A.S.C.E. Nov., 1960.

7. Metzner, A.B. Reed, J.C. — "Flow of Non-Newtonian Fluids- Correlation of laminar, transition and turbulent regions", Journal of A.I.Ch.E., Vol. 1, No. 4, Dec., 1950.

8. Alves, G.E. Boucher, D.F. Pigford, R.L. — "Pipe line Design- Non-Newtonian Solution and Suspensions"- Chemical Engineering Progress, Vol. 48, No. 8, August, 1952.

9. Brown, R.L. — "Designing Laminar flow Systems"- Chemical Engineering, June 12, 1961.

10. Dodge, D.W. Metzner, A.B. — "Turbulent flow of non-Newtonian Systems"- Journal of A.I.Ch.E., Vol. 5, No. 2, June, 1959.

11. Oldroyd, J.G. "Non-Newtonian flow of Liquids and Solids" in "Rheology- Theory and Applications"- Ed. Eirich, Academic Press Inc., N.Y., 1956.

12. Frisch, H.C. Simha, R. "The Viscosity of Colloidal Suspensions and Macromolecular Solutions" in "Rheology"- Ed. Eirich, Academic Press Inc., N.Y., 1956.

13. Metzner, A.B. Whitlock, M. "Flow Behaviour of Concentrated (Dilatant) Suspensions"- Trans. Society of Rheology, II, 1958.

14. Schack, C.H. Dean, K.C. Molloy, S.M. "Measurement and Nature of Apparent Viscosity of Water Suspension of some common minerals"- Report No. 5334, U.S.D.I. - Bureay of Mines.

15. Moreland, C. "Viscosity of Suspensions of Coal in Mineral Oil"-The Canadian Journal of Chemical Engineering, February, 1963.

16. Rutgers, Ir. R. "Relative Viscosity and Concentration"-Rheologica Acta, Band 2, Heft 4, 1962.

17. Rutgers, Ir. R. "Relative Viscosity of Rigid Spheres in Newtonian Liquids"- Rheologica Acta, Band 2, Heft 3, 1962.

18. Thomas, D.G. "Laminar Flow Properties of Flocculated Suspensions"- Journal of A.I.Ch.E., Vol. 7, No. 3, 1961.

19. Bagnold, R.A. "Experiments on a Gravity Free Dispersion of Large Solid Spheres in a Newtonian fluid under Shear"-Proc. Royal Society, London-Series A, Vol. 225, 1954.

20. Bagnold, R.A. "The Flow of Cohesionless Grains in Fluids"-Philosophical Transactions of the Royal Society of London, Series A, Vol. 249, 1956 - 57.

21. Arie Ram, Tamir, A. — "A Capillary Viscometer for Non-Newtonian Liquids" Industrial and Engineering Chemistry, Vol. 56, No. 2, February, 1964.

22. — "Symposium on Non-Newtonian Viscometry"-ASTM Special Technical Publication-No. 299.

23. Hiso Kada, Hanratty, T.J. — "Effects of Solids on Turbulence in a Fluid"-Journal of A.I.Ch.E. Vol. 6, No. 4, December, 1960.

24. Badger, W.L. Banchero, J.T. — "Introduction to Chemical Engineering"-McGraw-Hill Book Co. Inc., N.Y. 1955.

25. Graton, L.C. Fraser, H.J. — "Systematic Packing of Spheres" -Journal of Geology, Vol. XLIII, No. 8, Part 1, 1935.

APPENDIX A

TABLE: A - 1

CALIBRATION OF CAPILLARY TUBE: (A - M)

TUBE: A, LENGTH = 122 cm., DIA: 2mm

OIL: M, TEMP. = 72°F VISCOSITY: 4.416 c.p.

SP.GR.:0.8547

EXPT. NO.	VOL. c.c.	TIME secs	PRESS DIFF. cm. $H_m = \frac{\Delta p}{\rho g}$	τ_{wm} Dynes/cm^2	$\frac{8V}{D}$ sec^{-1}
1	43.0	65.3	141.0	48.5	840
2	47.9	71.6	141.0	48.5	870
3	42.0	29.1	295.0	101.5	1835
4	39.0	27.2	295.0	101.5	1830
5	46.5	28.3	340.0	115.0	2100
6	46.0	29.2	317.0	109.0	2000
7	45.0	25.1	365.0	125.5	2280
8	42.0	20.8	401.0	138.0	2580
9	41.0	17.9	459.0	158.0	2930
10	41.5	16.0	508.5	175.0	3310
11	42.0	12.8	670.0	230.0	4180
12	46.0	11.3	815.0	280.5	5200

TABLE: A - 2

CALIBRATION OF CAPILLARY TUBE: (A - N)

TUBE: A LENGTH = 122 cm. DIA = 2 mm.

OIL: N TEMP. = 71°F VISCOSITY = 9.017 c.p.

SP. GR. = 0.851

EXPT. NO.	VOL. c.c.	TIME secs	PRESS DIFF. H_m cm	τ_{wm} Dynes/cm^2	$\frac{8V}{D}$ sec^{-1}
1	42.0	123.4	136.5	46.7	433
2	39.0	52.1	304.0	104.0	955
3	47.5	46.5	422.0	144.0	1300
4	44.0	36.0	503.0	172.0	1555
5	41.8	28.3	585.0	200.0	1885
6	42.5	24.6	704.0	241.0	2200
7	41.8	20.4	825.0	282.0	2620
8	46.8	19.6	957.0	328.0	3040

TABLE: A - 3

CALIBRATION OF CAPILLARY TUBE: (B - M)

TUBE: B LENGTH: 118 cm. DIA: 2.7 mm.

OIL: M TEMP. = 72°F VISCOSITY: 4.416 c.p.

SP. GR. 0.8547

EXPT. NO.	VOL. c.c.	TIME secs	PRESS DIFF. H_m cm	τ_{wm} Dynes/cm²	$\frac{8V}{D}$ sec^{-1}
1	46.5	17.8	139.0	66.8	1350
2	46.5	14.4	170.5	81.8	1670
3	45.5	11.0	218.0	104.5	2140
4	43.0	8.9	261.0	125.0	2500
5	46.5	8.4	290.0	139.0	2860
6	44.0	5.6	421.0	202.0	4060
7	49.5	18.8	138.5	65.5	1360
8	45.0	17.0	139.1	67.0	1370
9	46.5	11.2	219.5	105.0	2150
10	45.0	8.1	295.0	142.5	2870
11	44.5	6.4	366.0	175.5	3590
12	85.0	7.8	458.0	220.0	4530
13	67.0	7.4	473.0	227.0	4690

TABLE: A - 4

CALIBRATION OF CAPILLARY TUBE: (B - N)

TUBE: B LENGTH: 118 cm. DIA: 2.7 mm.

OIL: N TEMP. = 72°F VISCOSITY: 8.872 c.p.

SP. GR. 0.8508

EXPT. NO.	VOL. c.c.	TIME secs	PRESS DIFF. H_m cm	τ_{wm} Dynes/cm^2	$\frac{8V}{D}$ sec^{-1}
1	45.5	34.7	141.5	68.0	679
2	43.0	17.2	261.0	125.2	1300
3	46.5	14.3	352.0	169.0	1680
4	40.0	9.9	433.0	208.0	2090
5	38.5	8.5	470.0	226.0	2350
6	43.5	8.2	559.0	268.5	2740
7	46.5	9.5	520.0	250.0	2540
8	49.0	14.4	358.0	172.0	1760
9	48.0	22.6	222.5	107.0	1100
10	48.0	35.3	140.5	67.5	705

TABLE: A - 5

SAND-WATER SUSPENSION TEST DATA - A.

SERIES: A D = 0.20 mm. α = 0.82 L = 122 cm.

$$\tau_\omega = 981 \times SG \times \frac{H_m}{L} \times \frac{D}{4} \times \alpha$$

$$\frac{8V}{D} = 8 \frac{\forall}{\frac{\pi}{4} D^2 t} \times \frac{1}{D}$$

EXPT. NO.	VOL. $\forall$ c.c.	TIME t sec.	DIFF. PRESS HEAD H_m cm.	CONC. C.	SP. GR. SG	τ_ω Dynes/cm^2	$\frac{8V}{D}$ sec^{-1}
A-1	43.5	18.6	166	0.125	1.205	65.9	2978
A-2	42.2	14.6	218	0.129	1.212	87.1	3680
A-3	44.0	12.0	310	0.129	1.212	123.9	4669
A-4	40.5	12.3	262	0.134	1.220	105.4	4192
A-5	44.5	10.55	381	0.134	1.220	153.2	5371
A-6	45.0	22.0	142	0.159	1.260	59.0	2600
A-7	44.5	18.3	185	0.159	1.260	76.8	3096
A-8	43.9	13.63	256	0.174	1.275	107.6	4101
A-9	35.0	11.80	228	0.201	1.330	100.0	3777
A-10	43.0	17.20	216	0.216	1.355	96.2	3183
A-11	37.5	19.70	164	0.226	1.370	741	2424
A-12	43.5	20.10	175	0.250	1.410	81.3	2756
A-13	43.0	9.90	490.5	0.271	1.445	233.7	5530
A-14	41.5	10.10	488	0.277	1.455	234.1	5232
A-15	41.6	8.65	559	0.278	1.455	268.1	6123

TABLE: A-5, continued

EXPT. NO.	VOL. $\forall$ c.c.	TIME t sec.	DIFF. PRESS HEAD H_m Cm	CONC. C	SP. GR. SG	τ_w Dynes/cm^2	$\frac{8V}{D}$ sec^{-1}
A-16	44.0	8.80	674	0.287	1.470	326.6	6366
A-17	47.5	48.60	178	0.299	1.490	87.4	1244
A-18	41.4	8.90	590	0.302	1.495	290.8	5923
A-19	44.8	10.80	524	0.305	1.500	259.1	5282
A-20	42.2	14.80	310	0.310	1.510	154.3	3630
A-21	40.0	19.8	291	0.317	1.520	145.8	2572
A-22	41.6	8.3	741	0.323	1.530	373.8	6382
A-23	35.0	103.4	134	0.326	1.535	67.8	471
A-24	31.0	58.6	208	0.332	1.545	105.9	674
A-25	32.0	102.8	134	0.335	1.550	68.5	396
A-26	33.0	103.2	134	0.335	1.550	68.5	407
A-27	34.0	38.3	382	0.335	1.550	195.2	1130
A-28	43.0	51.7	336	0.338	1.555	172.3	1059
A-29	41.0	58.6	348	0.341	1.560	179.0	892
A-30	43.5	47.2	399	0.341	1.560	205.2	1173

TABLE A - 5, continued

EXPT. NO.	VOL. $\forall$ c.c.	TIME t sec.	DIFF. PRESS HEAD H_m cm	CONC. C	SP. GR. SG	τ_w Dynes/cm^2	$\frac{8V}{D}$ sec^{-1}
A-31	29.1	100.9	134	0.342	1.562	69.0	367
A-32	43.0	37.8	465	0.342	1.562	239.2	1448
A-33	39.2	65.3	239	0.344	1.565	123.3	764
A-34	41.8	51.8	347	0.345	1.565	179.0	1027
A-35	38.0	48.7	316	0.349	1.572	163.8	994
A-36	35.5	92.7	150	0.353	1.580	78.1	488
A-37	34.2	71.5	186	0.353	1.580	96.8	609
A-38	32.5	95.6	134	0.357	1.585	70.0	433

TABLE: A - 6

SAND-WATER SUSPENSION TEST DATA - B

SERIES: B D = 0.27 cm. α = 0.90 L = 118 cm.

EXPT. NO.	VOL. $\forall$ c.c.	TIME t sec.	DIFF. PRESS HEAD Hm Cm	CONCN. C	SP. GR. SG	τ_w	$\frac{8V}{D}$
B-1	50.0	4.30	310	.136	1.220	190.5	6017
B-2	105.0	8.10	371	.151	1.250	234.2	6708
B-3	67.8	6.80	241	.164	1.270	154.0	5160
B-4	71.2	6.20	277	.164	1.270	176.0	5943
B-5	51.0	7.20	160	.166	1.275	102.6	3666
B-6	69.7	5.90	338	.182	1.290	220.2	6114
B-7	65.7	6.40	259	.184	1.300	170.0	5312
B-8	69.7	7.30	251	.187	1.305	165.4	4941
B-9	53.6	7.30	170	.189	1.310	112.2	3800
B-10	81.3	9.30	203	.192	1.325	135.8	4524
B-11	60.0	6.70	228	.194	1.315	151.4	4634
B-12	58.3	7.10	206	.196	1.320	137.3	4249
B-13	80.7	7.40	306	.196	1.320	204.0	5644
B-14	70.5	5.25	415	.199	1.327	278.0	6955
B-15	46.2	7.2	137	.204	1.335	92.7	3321

TABLE: A - 6, continued

EXPT. NO.	VOL. $\forall$ c.c.	TIME t sec.	DIFF. PRESS HEAD H_m Cm	CONCN. C	SP. GR. SG	τ_3	$\frac{8V}{D}$
B-16	78.7	13.65	139.5	.204	1.335	93.7	2984
B-17	44.0	7.60	140	.204	1.335	94.4	2996
B-18	81.3	12.0	167	.204	1.335	112.2	3506
B-19	44.4	3.50	380	.222	1.365	262.0	6565
B-20	61.3	11.00	137	.235	1.380	95.5	2884
B-21	69.5	10.80	158.5	.238	1.380	110.5	3330
B-22	40.5	5.00	231	.250	1.390	162.2	4192
B-23	46.5	6.30	179	.257	1.410	127.5	3820
B-24	61.0	8.70	193	.257	1.420	128.7	3628
B-25	82.7	9.20	241	.257	1.420	172.8	4650
B-26	81.5	7.95	295	.257	1.420	211.6	530.5
B-27	47.0	8.50	142	.259	1.425	102.2	2862
B-28	43.0	6.00	198	.262	1.430	143.0	3708
B-29	40.0	6.50	163	.263	1.431	115.6	3185
B-30	43.0	5.80	214	.268	1.440	155.6	3837
B-31	43.0	4.50	312	.280	1.460	230.0	4945
B-32	45.0	5.30	256	.283	1.465	189.4	4394
B-33	58.0	5.10	388	.283	1.465	286.1	5885
B-34	43.0	7.40	170	.292	1.480	127.1	3007

TABLE: A - 7

SAND-WATER SUSPENSION TESTS - A

SERIES: A D = 0.20 cm. ρ_f = 1.00 gm/cm^3 η = 1.0 centipoise

d = 0.022 cm. ρ_s = 2.64 gm/cm^3

EXPT. NO.	C ×100	λ From Fig. 23	τ_ω	$\frac{8V}{D}$	τ_s	$\frac{\tau_s \rho_s d^2}{\eta^2}$	$(\frac{8V}{D})\frac{\rho_s d^2}{\eta}$	$\frac{\tau_s}{\lambda}\frac{\rho_s d^2}{\eta^2}$
A-1	12.5	1.35	65.9	2978	36.12	462	380.6	342.2
A-2	12.9	1.39	87.1	3680	50.30	643	470.3	462.5
A-3	12.9	1.39	123.9	4669	77.21	987	596.7	710.0
A-4	13.4	1.44	105.4	4192	63.48	811	535.7	563.1
A-5	13.4	1.44	153.2	5371	99.49	1271	686.4	882.6
A-6	15.9	1.69	59.0	2604	32.96	421	332.8	249.1
A-7	15.9	1.69	76.8	3096	45.84	586	395.7	346.7
A-8	17.4	1.83	107.6	4101	66.49	850	524.1	464.4
A-9	20.1	2.10	100.0	3777	62.23	795	482.7	378.5
A-10	21.6	2.26	96.2	3183	64.37	823	406.8	364.1
A-11	22.6	2.37	74.1	2424	49.86	637	309.8	268.7
A-12	25.0	2.42	81.3	2756	53.75	687	352.2	283.8
A-13	27.1	2.95	233.7	5530	178.40	2280	706.7	772.8
A-14	27.7	3.04	234.1	5232	181.78	2323	668.6	764.1

TABLE A - 7, continued

EXPT. NO.	C ×100	λ	τ_ω	$\frac{8V}{D}$	τ_s	$\frac{\tau_s \rho_s d^2}{\eta^2}$	$(\frac{8V}{D})\frac{\rho_s d^2}{\eta}$	$\frac{\tau_s}{\lambda}\frac{\rho_s d^2}{\eta^2}$
A-15	27.8	3.06	268.1	6123	206.87	2644	782.5	864.0
A-16	28.70	3.1	328.6	6366	262.94	3360	813.6	1060
A-17	29.90	3.38	87.4	1244	74.96	958	159.0	283.4
A-18	30.20	3.45	290.8	5923	238.57	3049	757.0	883.7
A-19	30.50	3.50	259.1	5282	206.28	2636	675.0	753.1
A-20	31.00	3.58	154.3	3630	118.00	1508	463.9	421.2
A-21	31.70	3.72	145.8	2572	120.08	1535	328.7	412.6
A-22	32.30	3.83	373.8	6382	309.98	3962	815.6	1034.4
A-23	32.60	3.90	67.8	431	63.49	811	55.1	207.9
A-24	33.20	4.02	105.9	674	99.16	1267	86.1	315.1
A-25	33.50	4.05	68.5	396	64.54	825	50.6	203.7
A-26	33.50	4.05	68.5	407	64.43	823	52.0	203.2
A-27	33.50	4.05	195.2	1130	183.90	2350	144.4	580.2
A-28	33.80	4.12	172.3	1059	161.71	2067	135.3	501.6
A-29	34.10	4.20	179.0	892	170.08	2174	114.0	517.6
A-30	34.10	4.20	205.2	1173	193.47	2473	149.9	588.8
A-31	34.20	4.22	69.0	367	65.33	835	46.9	197.8

TABLE: A - 7, continued

EXPT. NO.	C ×100	λ	τ_ω	$\frac{8V}{D}$	τ_s	$\frac{\tau_s \rho_s d^2}{\eta^2}$	$(\frac{8V}{D})\frac{\rho_s d^2}{\eta}$	$\frac{\tau_s}{\lambda}\frac{\rho_s d^2}{\eta^2}$
A-32	34.20	4.22	239.2	1448	224.72	2872	185.1	680.0
A-33	34.40	4.25	123.3	764	115.66	1478	97.6	347.0
A-34	34.50	4.27	179.0	1027	168.73	2156	131.3	504.9
A-35	34.90	4.35	163.8	994	153.86	1966	127.0	451.9
A-36	35.30	4.45	78.1	488	73.22	936	62.4	210.3
A-37	35.30	4.45	96.8	609	90.71	1159	77.8	260.4
A-38	35.70	4.55	70.0	433	65.67	839	55.3	184.3

TABLE: A - 8

SAND-WATER SUSPENSION TESTS - B

SERIES: B D = 0.27 cm.

d = 0.022 cm.

EXPT. NO.	C x100	λ From Fig. 23	τ_ω	$\frac{8V}{D}$	τ_s	$\frac{\tau_s \rho_s d^2}{\eta^2}$	$(\frac{8V}{D})\frac{\rho_s d^2}{\eta}$	$\frac{\tau_s}{\lambda}\frac{\rho_s d^2}{\eta^2}$
B-1	13.60	1.45	190.5	6071	129.19	1651	775.8	1138.6
B-2	15.10	1.61	234.2	6708	167.12	2136	857.2	1326.7
B-3	16.40	1.73	154.0	5160	102.40	1309	695.4	756.6
B-4	16.40	1.73	176.0	5943	116.57	1490	759.5	861.2
B-5	16.60	1.75	102.6	3666	65.94	843	468.5	481.7
B-6	18.20	1.91	220.2	6114	159.06	2033	781.3	1064.3
B-7	18.40	1.94	170.0	5312	116.88	1494	678.9	770.1
B-8	18.70	1.96	165.4	4941	115.99	1482	631.5	756.1
B-9	18.90	1.98	112.2	3800	74.20	948	485.6	478.7
B-10	19.20	2.00	135.8	4524	90.56	1157	578.2	578.5

TABLE: A - 8, continued

EXPT. NO.	C ×100	λ	τ_ω	$\frac{8V}{D}$	τ_s	$\frac{\tau_s \rho_s d^2}{\eta^2}$	$\frac{8V}{D} \cdot \frac{\rho_s d^2}{\eta}$	$\frac{\tau_s}{\lambda} \cdot \frac{\rho_s d^2}{\eta^2}$
B-11	19.40	2.03	151.4	4634	105.06	1343	592.2	661.5
B-12	19.60	2.05	137.3	4249	94.81	1212	543.0	591.2
B-13	19.60	2.05	204.0	5644	147.56	1886	721.3	920.0
B-14	19.90	2.09	278.0	6949	208.51	2665	888.0	1275.1
B-15	20.40	2.14	92.7	3321	59.49	760	424.4	355.1
B-16	20.40	2.14	93.7	2984	63.86	816	381.4	381.3
B-17	20.40	2.14	94.4	2996	64.44	823	382.9	384.5
B-18	20.40	2.14	112.2	3506	77.14	986	448.1	460.7
B-19	22.20	2.34	262.0	6565	196.95	2517	839.0	1075.6
B-20	23.50	2.47	95.5	2884	66.66	852	368.6	344.9
B-21	23.50	2.47	110.5	3330	77.20	987	425.6	399.5
B-22	23.80	2.50	162.2	4192	120.28	1537	535.7	614.8
B-23	25.00	2.67	127.5	3820	89.30	1141	488.2	427.3
B-24	25.70	2.76	128.7	3628	92.42	1181	463.7	427.8

TABLE: A - 8, continued

EXPT. NO.	C ×100	λ	τ_ω	$\frac{8V}{D}$	τ_s	$\frac{\tau_s \rho_s d^2}{\eta^2}$	$(\frac{8V}{D})\frac{\rho_s d^2}{\eta}$	$\frac{\tau_s}{\lambda}\cdot\frac{\rho_s d^2}{\eta^2}$
B-25	25.70	2.76	172.8	4635	126.45	1616	592.4	585.5
B-26	25.70	2.76	211.6	5305	158.55	2026	678.0	734.0
B-27	25.90	2.78	102.2	2862	73.58	940	365.8	338.1
B-28	26.20	2.82	143.0	3709	105.91	1354	474.0	480.1
B-29	26.30	2.84	115.6	3185	83.75	1070	407.0	376.7
B-30	26.80	2.90	155.6	3837	117.23	1498	490.4	516.5
B-31	28.00	3.09	230.0	4945	180.55	2307	632.0	746.6
B-32	28.30	3.14	189.4	4394	145.46	1859	561.6	592.0
B-33	28.30	3.14	286.1	5885	227.15	2903	752.1	924.5
B-34	29.20	3.28	127.1	3007	97.03	1240	384.3	378.0

APPENDIX B

APPENDIX - B

RELATIONSHIP BETWEEN λ AND C.

Consider an array of spheres of diameter d in a known type of piling, packed such that minimum amount of voids corresponding to the chosen piling are produced.

Let $\forall_s$ = Volume of Solids

$\forall$ = Total Volume

$C_* = \frac{\forall_s}{\forall}$ = Volume Concentration of Solids.

In this packing, since the amount of voids is minimum, the free distance between adjacent spheres is zero and hence by definition (Sec. 2.3) $\lambda = \infty$. Hence C_* is the concentration at $\lambda = \infty$.

Now let the distance between the adjacent spheres be increased to bd, keeping the piling arrangement the same.

In a total volume of $\forall$, the amount of solids present is now $\frac{\forall_s}{b^3}$. The resulting concentration of solids is

$$C = \frac{\forall_s}{b^3 \forall} = \frac{C_*}{b^3} \qquad \text{- - - - - - (B-1)}$$

But from Fig. 5, $bd = a + d$

$$b = \frac{a}{d} + 1$$

$$= 1/\lambda + 1 \qquad \text{- - - - - - (B-2)}$$

$$C = \frac{C_*}{\left(\frac{1}{\lambda} + 1\right)^3}$$

or

$$\lambda = \frac{1}{\left(\frac{C_*}{C}\right)^{1/3} - 1} \qquad \text{- - - - - - (B-3)}$$

In the above Equation B-3 , C_* is the maximum possible concentration of spheres in a given type of piling. The value of C_* for various types of pilings has been calculated by Slichter (25). It is found that the least valve of C_* is 0.524 for cubic piling and the greatest value of $C_* = 0.74$ for rhombohedral piling. Bagnold (20) has found $C_* = 0.65$ for natural uniformly rounded sand grains under dry compaction.

Fig. 23 shows the relationship between λ and C Calculated from equation B-3 with $C_* = 0.65$. This Fig. is used in the calculation of λ corresponding to various values of C in Tables A-7 and A-8.

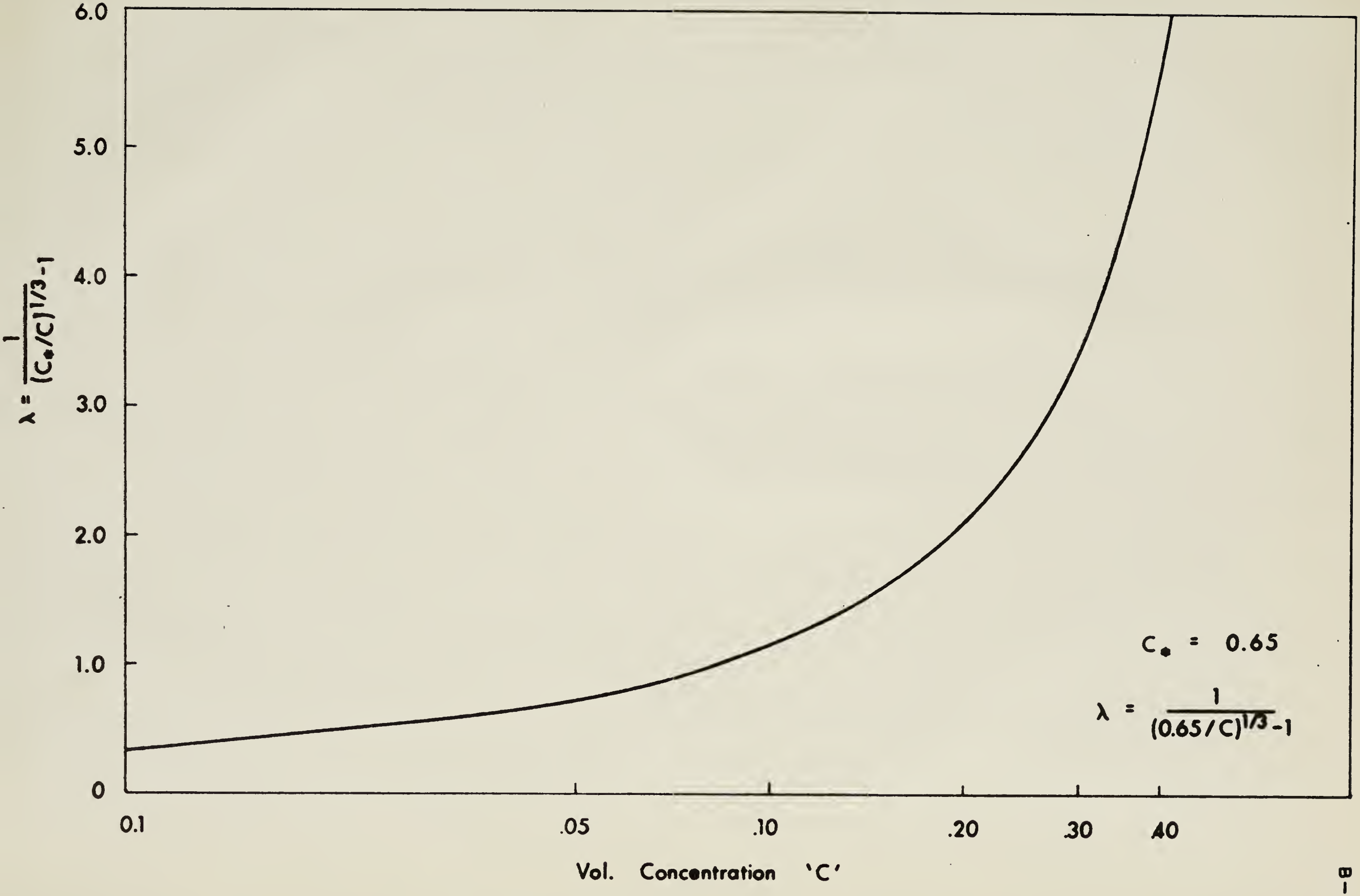

B-13

Fig. 23 Variation of λ with C